Structure and Thermodynamics of Polyelectrolyte Complexes

Johannes Frueh, Meiyu Gai, Simon Halstead and Qiang He

Abstract Polyelectrolytes (PEs) find applications in many fields of modern life starting from food additives to flocculation and solubility enhancers, down to viscosity adjusting agents in cosmetics and subterranean gelling or drug delivery agents. Most of these properties are related to the PE charge density, structure, counterions, temperature or counter PE. This book chapter gives an overview of the current state of understanding of the thermodynamical properties of PEs in solution. The theoretical predictions and results are compared with current state of the art computer simulations (with a focus on molecular dynamics) as well as experiments on PE structure, complex formation and viscosity properties.

Nomenclature

e	Valence of PE monomer group
k_BT	Thermal energy
k_B	Boltzmann constant
ε	Dielectric constant
ε_L	Local dielectric constant
l_D	Debye length
k	Inverse Debye length
l_0	Persistence length
l_B	Bjerrum length
l_M	Length between two monomers

J. Frueh (✉) · M. Gai · Q. He (✉)
Key Laboratory of Microsystems and Microstructures Manufacturing, Ministry of Education, Micro/Nano Technology Research Centre, Harbin Institute of Technology, Yikuang Street 2, Harbin 150080, China
e-mail: Johannes.frueh@hit.edu.cn

Q. He
e-mail: qianghe@hit.edu.cn

S. Halstead
School of Chemical Engineering and Technology, Harbin Institute of Technology, Xi Da Zhi Street, Harbin 150001, China

Visakh P.M. et al. (eds.), *Polyelectrolytes*, Engineering Materials,
DOI 10.1007/978-3-319-01680-1_2

l_d	Length of dipole
L	Length of fully elongated PE
L_C	Length of collapsed PE
L_ξ	Correlation length
L_M	Distance between 2 PE chain centers
L_str	Length of string between globules
L_ξ	Size of a globule/bead
c_S	Salt concentration
c_P	PE concentration
c^*	Crossover concentration
c_I^{loc}	Local concentration of counterions next to PE
f	Fraction of charged monomers
a	Monomer length/diameter
K	Reduced coupling constant (Based on thermal energy)
K'	Reduced coupling constant (based on excluded volume)
v	Excluded volume per monomer
v_0	Local volume close to monomer
$\bar{a}$	Elongation per monomer
ζ	Size of electrostatic blob
V_ζ	Volume of electrostatic blob
R	Total length of PE
R_H	Hydrodynamic radius
N	Number of monomers
n^*	Number of charged groups in PE
N_M	Number of monomers in the diameter D of a rodlike molecule
$N_M sr$	Number of monomers in string
$N_M bead$	Number of monomers in a bead
N_E	Number of monomers in entangled region
N'	Number of P-bonds in strong PE
N_2	Amount of PE molecules
N_1	Amount of solvent molecules
$N_1 i$	Amount of solvent molecules inside v_0
$N_1 o$	Amount of solvent molecules outside v_0
N_C	Number of counter ions
n_Ψ	Number of ψ bindings
D	Effective diameter of the rod-like molecule
d	Degree of dissociated charges
M	Mol
L	Liter
b	Charge density
n	Valence of counterions
k	Reaction constant
v_1	Volume fraction of solvent
v_2	Volume fraction of PE

v_3	Volume fraction of counterion
v_l	Molecular volume of solvent
v_c	Molecular volume of counterion
v_{PE}	Molecular volume of PE
V_l	Molar volume of solvent
V_2	Molar volume of PE
x	Number of gratings used in Flory lattice
ΔH	Free enthalpy
H_e	Electrostatic enthalpy
ΔS	Free entropy
S_M	Entropy of mixing
S_K	Kuhn entropy
S_C	Counter ion entropy
F_e	Free energy of electrolyte
F_A	Free energy of ionic atmosphere
F_0	Non electrostatic part of free energy
F	Free energy
χ	Flory Huggins solution parameter
E	Electrostatic based energies
E_D	Debye electrostatic energy of the PE chain
E_a	Energy of the counterion adsorbed on the PE
E_{ela}	Elastic energy of the stretched, charged PE
β	Fraction of free counter ions
β_c	Fraction of condensed counter ions
u	Charge density parameter
k_1	Constant related to k_2
k_2	Concentration parameter $\sim -\log c_P$
λ	Charge density parameter
z_e	Euler number e^x
e_e	Electron charge
Z_1	Effective expansion factor
W	Strength parameter for short ranged effects
A	Å
V_+	Positive ion cloud scaling factor
V_-	Negative ion cloud scaling factor
R_G	Ideal gas constant
F_1	Entropy of condensed counterions
F_2	Translational entropy of ions
F_3	Fluctuations between PE and ions
F_4	Ion pair energy
F_5	Free energy term for partly charged PE
F_6	Correlation term (ion pair PE)
η_s	Viscosity of the solvent
η	Viscosity of the solution

τ_{RZ}, τ_{RR}	Zimm and Rouse relaxation time
τ	Time
D_i	Diffusion coefficient
D_Z, D_R	Zimm and Rouse diffusion coefficient
Z_P	Friction coefficient of the polymer
Z_B	Friction coefficient of the beads
σ_s	Shear stress
$\dot{\gamma}$	Shear rate
β_R	Reduced shear rate
ϕ	Volume fraction
L_a	Tube diameter
T_R	Reduced temperature
θ	Theta temperature of solvent/PE
X	Concentration dependent parameter, which depends on concentration (values used for X are shown below the equations)

1 Introduction

Polyelectrolytes (PEs) are polymers with charged monomer groups that can dissociate into a charged macroion and small counterions when the PE is dissolved in a polar solvent [1, 2]. These charged polymers are, in many cases, employed in nature, and not only DNA [3] but also proteins and cellulose can be classified as PEs [1]. Technical applications of PEs include, for example, PE-DNA drug delivery complexes called polyplexes [4, 5]. PEs are also frequently used in industry. For example, polyethylenimine (PEI) is used in wastewater treatment [6], or biodegradable PEs like dextransulphate and gelatin PE are used in food science [7]. For the past 20 years, PEs have also been used to fabricate nanofilms [8] and nanostructures [9], called polyelectrolyte multilayers (PEM) which are now being introduced into common products [6]. Due to the existence of excellent review papers on the broad field of cellulose, which is used in the fields of food, medicine, paper, cosmetics, viscosity adjustment and clothing, we omit most of the applications of this type of PE and refer to the other excellent reviews and publications [10–13].

Other fields of application for PEs, which especially rely on the viscosity, are drilling and fracking [14]. In these fields a controlled gelation point and gelation times are also necessary [14]. Due to the growing importance of this field, the basics of this field will also be discussed and references given.

Although PEs and PE solutions have been investigated for a long time [2, 15], a clear understanding of PEs has only emerged within the last decade [16]. The reason that the understanding of this kind of polymer has taken so long is due to the fact that the interaction between charged groups (which can be additionally shielded by counterions), hydrophobic forces and hydrogen bonds occur at the

same time [1]. This interplay between forces leads to several interesting effects of PE solutions which include:

1. Decreasing viscosity upon increasing PE concentration for some strong PEs, whereas the viscosity increases in the case of neutral polymers [2, 17].
2. Formation of electrostatic and Gaussian blobs, necklace-like structures or linear rods, depending on the solvent quality and PE charge [2, 18].
3. Formation of complexes with oppositely charged PEs [19].
4. Due to the release of counterions, the osmotic pressure of PEs is much higher than that of neutral polymers [16].
5. Crossover from dilute to semidilute concentration regions occurs at lower concentrations than in the case of neutral polymers [16].
6. Due to the emerge of regular PE structures in homogeneous solutions, the PE solutions exhibit a peak in the scattering function [2], the intensity of which correlates with $C^{1/2}$ of the PE concentration [16]. In the case of neutral polymers, the lack of regular structure prevents such a peak [16].

This book chapter contains a review of the current state of research in the field of the thermodynamics and viscosity of PEs in solution. In Sect. 2 an overview of the coupling constants in the PE, defining the degree of electrostatic interaction between the PE ionic groups is given. It also contains a review of the interaction and coupling strength between the PE ionic groups and their counterions, and gives definitions of weak and strong PEs. Section 3 reviews the enthalpy of PEs and PE complexes in solution, and Sect. 3.1 contains an overview of the Flory-Huggins solution parameter, which is based on mean field theory and is frequently used to estimate the solution enthalpy and solvent quality. In subsequent parts, this section contains an introduction of enthalpy driven processes that mainly occur in weak PEs. In contrast to weak PEs, entropic processes are the driving force in the case of strong PEs. Section 3 closes with a discussion of the thermodynamic properties of PE complex formation.

Recent results of computer simulations and structure determinations are summarized in Sect. 4. Since Monte Carlo simulations will be reviewed in Sect. 4.1, only a short abstract of the recent state of research of this simulation method relevant to the chapter can be found in Sect. 4.1, along with recent developments in the polymer field theory which has made big advances recently. The recent state of molecular dynamics simulations (Sect. 4.2) is the main focus of Sect. 4.

The experimental results in Sect. 5 are also compared with the simulation methods and thermodynamic calculations. The viscosity and rheology measurements in Sect. 5.1 are the focus of the experimental section, with additional contributions of scattering measurements for PE structure determination in Sect. 5.2 and spectroscopic measurements in Sect. 5.3.

Regarding the layout of each chapter except Sect. 6, it is worth noting that each chapter is structured in such a way that first the PEs are evaluated in solution and then the PE complexes are discussed. Since PE multilayers (and 2D PE complexes) have been reviewed extensively [6, 16, 20], they are only mentioned

briefly in this book chapter and the focus of this chapter is shifted to 0 dimensional gels and dissolved PE complexes. Osmotic pressure and conductivity measurements are omitted in this chapter.

PE complexes and gel properties are mentioned in each section, and their explicit properties and applications are summarized in Sect. 6. For convenience, this book chapter focuses on summarizing the basic properties of PEs. For readers convenience several excellent review papers are cited and recommended for further reading.

2 Weak and Strong Electrostatic Coupling

The interaction and structure of PEs in a solvent (mostly water) are controlled to a large extent by electrostatic interactions [2, 15, 21]. In case of PEs in the strong dilution regime, this interaction leads to an intramolecular charge repulsion and to strongly extended, rod like chains [2]. For this reason the Bjerrum length, l_B, which defines the distance at which the electrostatic interaction reaches the same value as the thermal energy (k_BT), is an important parameter [21]:

$$l_B = \frac{e^2}{k_BT \cdot 4\pi\varepsilon} \tag{1}$$

In (1) ε is the dielectric constant of the solvent (in water ($\varepsilon \sim 78$) l_B is $\sim$7 Å [21]), and e is the monomer charge. If a PE is dissolved in a salt solution, the charges of the PE are further screened by the ions of the salt, and the interaction strength decays with the Debye length l_D [21]. $l_D = k^{-1}$, with $k = 8\pi c_s l_B$, with c_S being the salt concentration [21]. Compared to uncharged molecules which can be described by simple Gaussian statistics [21], the intramolecular charge repulsion causes an increased persistence length, l_P (a value that defines the stiffness of a polymer). If l_0 is the persistence length of an uncharged chain, the persistence length of a PE in salt solution becomes [21]:

$$l_P = l_0 + \frac{\tau^2 l_B}{4k^2} \tag{2}$$

with $\tau = f/a$, where the fraction of charged monomers are f, and a is the monomer length [2, 21, 22]. The interaction between the polyelectrolyte monomer groups is dependent on the charge density [2]. Some groups, like the R-COOH groups of polyacrylic acid (PAA), show a charge density depending strongly on the pH and are therefore regarded as "weak" polyelectrolytes [21]. In contrast, PEs that carry monomer groups that are almost unaffected by the pH, like the sulphonate group of polystyrenesulphonate (PSS), are considered "strong" polyelectrolytes [15, 21]. One of the first authors who introduced the idea of a coupling constant to describe

the interaction of PEs with each other and the surrounding was nobel laureate De Gennes [22]. In earlier methods like those of Kuhn et al. [2] or Overbeek [23] the average charge density or directly the free energy was used. The scaling method of De Gennes [22], who used the Rouse as well as the Zimm methods for describing the interaction in polyelectrolyte solutions, is the focus of this section [24–28]. The degree of interaction of these electrostatic groups with each other in the same PE [3, 15, 22], with counterions [3, 15, 22], and with oppositely charged PEs is often described by the reduced coupling constant K [22]:

$$K = l/a \tag{3}$$

with a being the monomer unit length and l being the characteristic length, according to Ref. [22]:

$$l = \frac{e^2}{\varepsilon k_B T} \tag{4}$$

Another "reduced" coupling constant, is defined by the excluded volume of one monomer length v and the actual volume of the monomer [18, 22, 29]:

$$K' = \frac{v}{a^3} \tag{5}$$

Both reduced coupling constants have in common, that they rely on a volume that excludes same charges. $K \geqq 1$ leads to a condensation of counterions on the polyelectrolyte [22]. The coupling constant depends strongly on the type of investigated PE. For this reason PEs can be divided into two main groups.

2.1 Weak PEs with Weak Electrostatic Coupling Constants

In case of a weak coupling, the coupling constant, K, is far below 1 (please note that in some old papers other nomenclature is used) [2, 22]. Due to the weak coupling constant, the elongation (due to electrostatic repulsion) as well as the persistence length of the molecule is quite low [2, 22]. Therefore the average elongation per monomer unit, $\bar{a}$, due to the electrostatic repulsion force, F, is defined according to de Gennes [22]:

$$\bar{a} = F\frac{a^2}{3T} \tag{6}$$

The weak elongation of the monomers leads to the evolution of so-called electrostatic blobs [2, 18, 22] of blob size ζ [22] in which the PE chain is randomly

oriented. In some cases the chain structure might be rod-like due to an array of blobs with the blob size being the diameter of the chain [18, 22, 29].

$$\zeta \sim a\left(\frac{1}{K}\right)^{1/3} \tag{7}$$

The resulting polymer chain with N monomers and a total chain length R [22, 30] is:

$$R \sim N\zeta\left(\frac{\ln(N)}{3}\right)^{1/3} \tag{8}$$

The blob size correlates with the number of monomers, N_M, in the blob and so, according to de Gennes [18, 26, 29, 30] ζ may be calculated by:

$$\zeta \sim a\sqrt{N_M} \tag{9}$$

At this point it is worth pointing out that other authors use different definitions and models to define a blob, like thermal blobs (that are also called globules or electrostatic blobs), or beads in a necklace model. For a detailed review about these models and structures see references [26, 30]. It is also important to note, that a real PE chain is swollen in solvent and therefore the blob (or effective diameter) size in a real system is larger than in theory [30]:

$$\zeta_{real} \sim a(N_M)^{3/5} \tag{10}$$

Since the electrostatic blobs experience a concentration and solvent dependent repulsion as well as an attraction due to hydrophobic interaction and counterion condensation, the PE concentration dependent correlation length, D, was introduced by de Gennes [22]. This correlation length depends on the length of the PE, the concentration of the PE (c_P) used and the concentration at which the PE blobs start to overlap (c^*), which is known as the crossover concentration. The calculation was developed for cases when $c_P \gg c^*$, where D can be interpreted as a region without chain overlap (intra as well as intermolecular) [22, 26, 30].

$$D = L\left(\frac{c^*}{c_P}\right)^{1/2} = \left(\frac{1}{c_P a}\right)^{1/2} \tag{11}$$

The scaling of D is similar to the Debye length. At low concentrations $(c_P \ll c^*)$, the correlation of the screening length due to counterions is the Debye length l_D [22, 29]. The relation of c_P to the polymer-polymer distance d is $c_P = \frac{2N}{d^3}$ [22, 29]. At very low concentrations, the screening length can be larger than the polymer length.

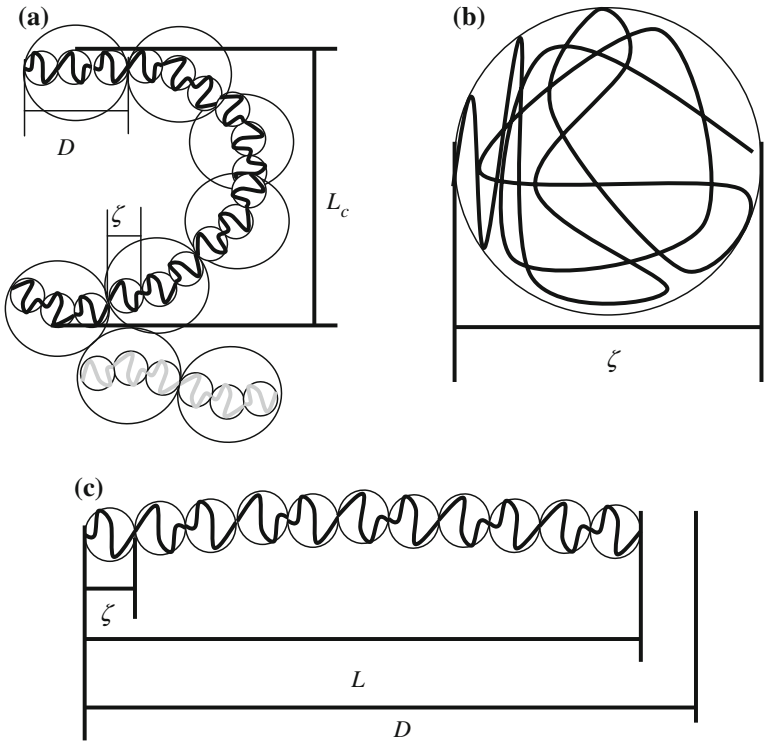

Fig. 1 Illustration of the PE conformation with different coupling and charge repulsion conditions, according to de Gennes. ζ is the blob size, D is the correlation length and L is the length of the polymer, where L_C symbolizes the length of the collapsed polymer chain **a** $\zeta < D < L$ and the polymer chain might exhibit a random walk of correlation of the blobs and the orientation of the chain diameter D, black: chain 1, gray: chain 2 **b** very weak electrostatic interaction ($\zeta > L > D$) the chain is in a Gaussian coil-like formation similar to an uncharged chain. **c** $\zeta < L < D$, strong repulsion of same charges, the chain is strongly elongated. The drawing style of the figure was inspired from Ref. [31]

As a result of the theory of de Gennes [16, 22, 29, 30], the structure of the PE is highly dependent on the coupling constant and the repulsion of the electrostatic blobs. The three parameters D, ζ and R behave strikingly differently depending on the solvent quality, electrostatic charge or the coupling constant. In the case of strong shielding of the charges so that $\zeta < D < L$, the polymer chain exhibits a random walk of correlation of the blobs and the orientation of the chain within the diameter, ζ, is Gaussian (see Fig. 1a). In such a case, the length of the polymer is collapsed and therefore shorter than the length of the elongated polymer, and can be calculated according to following equation [16, 22]:

$$L_c = N_M a \left(\frac{c^*}{c_P}\right)^{1/4} \sim \sqrt{N} K^{1/4} \tag{12}$$

If the solvent is very poor and the electrostatic forces are very weak or strongly shielded ($\zeta > L > D$), the whole chain is in a Gaussian coil-like formation similar to an uncharged chain (see Fig. 1b). In case of a very strong electrostatic repulsion with $\zeta < L < D$, the chain is strongly elongated, as shown in Fig. 1c.

The above formulas and theories were proven experimentally by X-ray and neutron scattering [22], with rheology [2] and spectroscopic measurements in the form of a pyrene labeled PE [32–35]. A summary of these experiments is presented in Sect. 5.

2.1.1 Strong Polyelectroyes with a Strong Electrostatic Coupling Constants

Recent reviews and simulations mainly focus on weak PEs [16, 26, 30], and this is mainly due to the complexity of counterion condensation and computational limits. For this reason this section summarizes the original work of Osawa and Manning (famous for the Osawa-Manning counterion condensation parameter $\gamma = l_B b$, with b being the charge density) [26], but also mentioning recent studies, of Muthukumar.

Strong PEs are, in contrast to weak PEs, insensitive to the surrounding pH. Examples of this type of PE are polystyrenesulphonate (PSS) and polydimethyldiammonium chloride (PDDA). In contrast to weak electrostatic coupling in weak PEs, strong electrostatic coupling between the ionic groups and their counterions $K \geqq 1$ leads to a concentration dependent condensation of counterions [3, 15, 22]. The interactions of a strong PE along, with the condensation of counterions on the PE, were mainly determined by Osawa and Manning [3, 15]. Counterions that condense on the PE can, according to Osawa and Manning be separated into two major interaction types, namely [3, 15, 36, 37]:

1. π-binding of counterions that are condensed and do therefore not contribute to the coulomb interaction
2. Ψ-binding of counterions that can freely move in solution and that contribute to the coulomb interaction.

According to Osawa (later proven by Manning and others [3, 36]), the counterions within an electrostatic blob are considered inactive, while those outside of the blob are considered active [15, 36, 38]. To estimate the relative amount of the two binding types and therefore the structure of the PE, one can use a simplified relation of the correlation between the blob volume, V_ζ, and the concentration of the added salt. For the precise version of (13), see Ref. [15].

$$V_\zeta \approx \frac{1}{\sqrt{c_S}} \tag{13}$$

Relation (13) is only valid in the case of low amounts of monovalent ions. To distinguish between π and Ψ bonds, the reaction constant of the ionic binding can

be calculated. The Ψ binding reaction constant, k, scales inversely to the blob volume [15].

$$k = \frac{\alpha}{1-\alpha} \cdot \frac{n_\Psi}{V_\zeta} \tag{14}$$

where the second term in Eq. (14) denotes the average concentration of Ψ bonds with n_Ψ being the number of Ψ bonds. The value of n_Ψ can be measured e.g. via the osmotic pressure of the solution. α defines in (14) the fraction of π bonds, where $\alpha = N'/N_M$. Since N' and (14) depend strongly on the ionic strength, N' is calculated as a function of the ionic strength of the solution [15]. If $N'/N_M < 0.1\ M/L$ then α is close to unity [15]. If large amounts of salt are added, then the value of α decreases drastically.

An interesting finding, made in 1954 by Osawa, was that the amount of Ψ bindings decrease with increasing ionic strength [see Eq. (15)]. For the precise version, see Ref. [15]), which correlates with viscosity measurements [15].

$$\Psi \approx \ln \frac{1}{c_S} \tag{15}$$

In case of multivalent (including monovalent) ions, the correlation between the valency of the counterion and the structure of the PE was mainly investigated by Manning [3] and, in recent years, also by Muthukumar [36]. According to Manning [3], the structure parameter, ξ, and the charged fraction of the PE, τ, are:

$$\xi = \frac{q^2}{\varepsilon k_b T b} \tag{16}$$

$$\tau = (n\xi)^{-1} \tag{17}$$

where b is the charge density and n is the valency of the counterions. In the case of DNA in a 0.5 M magnesium ion solution, 50 % of the phosphate groups of the DNA are shielded by counterions [3], compared to only 4 % in case of monovalent ions [3]. The local concentration of the counterions, c^{loc}, depends only on the structure parameter and on the local charge but not on the PE concentration [3].

$$c^{loc} = 24.3 \cdot \left(\xi b^3\right)^{-1} \tag{18}$$

It was also pointed out by Manning that at $c_S \sim c^{loc}$ the binding of the counterions might become very weak but, due to the low concentrations required for the experiment, measurements were difficult at his time [3]. Such a surprising and counterintuitive finding is in agreement with a recent study, investigating the structure of pyrene labeled PSS at very low concentrations in a salt free solution with fluorescence spectroscopy [33, 39, 40]. In these studies, pronounced coiling of the PEs was found even at very low concentrations and in absence of added salt [39].

Such findings are also in agreement with the theory of Muthukumar [36], which assumes a different dielectric constant close to the PE compared to the bulk. For concentrations higher than c^{loc}, the relations have been proven not only by X-ray and neutron scattering, including corresponding simulations [22, 38], but also with rheology [2] and spectroscopic measurements in form of pyrene labeled PE [32, 39, 41] and EPR spectroscopy [42] (see also Sect. 5).

3 Thermodynamics of Polyelectrolytes and Polyelectrolyte Complexes

In contrast to apolar polymers, the solution behavior of which can be readily explained by the Flory-Huggins theory [43–45], the thermodynamics and solution behavior of PEs is a little more demanding. This is due to the contributions of charged groups, as well as charged group-solvent and additional ion effects [3, 16, 26]. Additionally, the different coupling levels between weak and strong PEs makes the theoretical treatment demanding [29]. For this reason, the following section introduces several approaches used to describe the observed phenomena.

The Flory-Huggins theory (a mean field based approach) and statistical thermodynamic approaches based on the Debye-Hückel theory are the two most frequently used approaches. In the Debye-Hückel approach, the interactions between charges of the same sign cause intramolecular self-repulsion influencing the PE interaction and structure.

The Flory-like approach is based on mean field theory and solvent quality, where a good solvent causes a extended coil and a bad solvent causes phase separation (intra and intermolecular, concentration dependent). The Flory-like approach was used in two ways: in the classical way where charge fraction is neglected and just the solution parameter χ is used; and the modified theory, which contains chain length and charged fraction. The approaches are discussed separately in the following sections, which also contains some new approaches at the end of each section. The enthalpy and entropy of strong and weak PEs are considered separately, since the complex formation and solution behavior depends strongly on the coupling constant.

3.1 Flory-Huggins Solution Theory Applied to Polyelectrolye Solutions

The thermodynamics of dissolved apolar polymer systems is usually described by the Flory-Huggins theory [43–45]. The Flory-Huggins theory is based on the so called mean field approach which is a theory that assumes, that each part of the monomer-monomer interaction and solvent-solvent interaction has the same

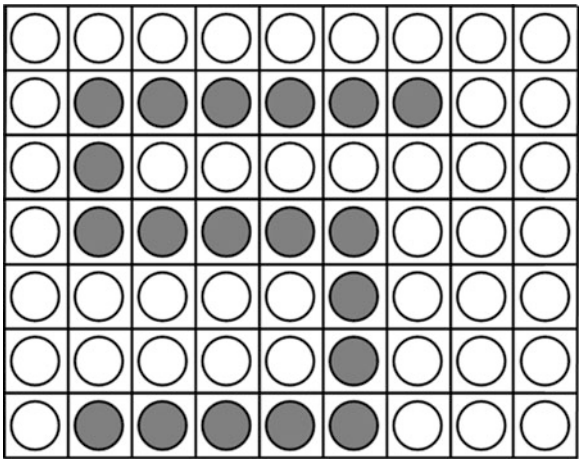

Fig. 2 A graphical visualization of the Flory-Huggins mean field theory. The grating positions with *white circles* illustrate the *solvent* and the *gray circles* illustrate the PE. It's assumed that: Each field has the same size, no overlap of fields or chains, all field positions are occupied, all polymer-polymer interactions are the same (all chain parts are the same)

energy (PE is not a co-polymer), no overlap of the chains is possible and fluctuations are neglected, see Fig. 2 [43–46]. This theory can therefore not directly forecast electrostatic blobs. The approach of averaging over all PE monomer site, allows forecasting solution qualities or general interactions. It is therefore possible to indirectly predict such blobs and the coiling of the molecule via the solvent quality (although Kuhn did not know of the work of Flory, he used a similar approach based on charged fractions and polar solvent) [2, 26]. According to Flory [44] the entropy of mixing for apolar molecules is:

$$\Delta S = k_B[N_1 \ln v_1 + N_2 \ln v_2] \tag{19}$$

where k_B is the Boltzmann constant, N_1 and N_2 are the number of solvent and polymer molecules, and v_1 and v_2 are the volume fractions of the monomers. The enthalpy of mixing, ΔH, for an apolar polymer is, according to Flory [44]:

$$\Delta H = \frac{BN_1N_2V_1V_2}{N_1V_1 + N_2V_2} \tag{20}$$

Here B is a constant, and V_1 and V_2 are the molar volumes where $V_2 = V_1 \cdot x$, with x being the amount of used grating places in the lattice. Despite the Flory-Huggins theory being originally developed for apolar molecules, it was used successfully to describe the swelling of PE complexes in the form of PEM thin films at different humidities [47]. In this study the PEM was considered to be a polymer matrix with the PE charges being compensated. Therefore, only the total interaction of the PE with the solvent was of interest and could therefore be

estimated with the Flory-Huggins solution parameter [47]. Another study (currently in preparation for publication) used the Flory-Huggins solution parameter as well as (19) and (20) to estimate the enthalpy and entropy of elongated PEM thin film complexes. The molecular image of the behavior of such complexes upon macroscopic elongation is that the electrostatic blobs decoil [39]. Such an approach is also successful in explaining the increased hydrophilic behavior of PEM upon mechanical load [48]. The Flory-Huggins solution parameter was also used successfully by other groups to calculate the dilution enthalpy, as well as the excluded volume and elastic energy of the PE chains for chitosan and alkylchitosan [49].

A completely new approach for the simulation of PE solutions was published by Katz and Leibler in 2009, not by using the Flory-Huggins solubility parameter of the polymer backbone, but instead using the one of the counterions [50]. The concept is logical and overdue, since the solubilization of a PE is caused by the release of the counterions and the resulting gain in entropy. Katz and Leibler were able to show all features observed up to now, such as phase separation, meso- and macro-phases and also the calculation of mixing ratio, depended on structure factors [50].

Alternatively to the work of the Flory-Huggins theory, other methods like the Hansen solubility parameter can be used to estimate the solvent quality [51]. In the Hansen approach, the polar, hydration, and dispersion components are considered separately and the contribution of each parameter is considered [46, 51, 52].

An interesting alternative to the Flory-Huggins or other mean field approaches was a study done by Pfeuty using a zero point Langrangian theory and between 1 and 6 dimensions [53]. In this study the authors found a deviation of the asymptotic properties of for high molecular weight PE chains between Flory type calculations and Lagrangian calculations. The authors, however, did not state a comparison with experimental values and the study was not frequently cited in other following reviews [16, 26, 30]. In 1999, Tsonchev et al. published a lattice field approach based on a corrected mean field theory to determine the patrician function, electrical potential, monomer distribution and other thermodynamic parameters such as the free energy [54]. Their approach presented reasonable results for all the variables tested.

3.2 Enthalpy in Polyelectrolyte Solutions

In this section the solution and mixing enthalpy of PEs are reviewed, with weak and strong PEs being reviewed separately due to the mechanics of structure and complex-formation differing greatly between these two types of PE.

3.2.1 Dilution, Mixing and Solution Enthalpy of Weak PEs

Weak PEs are, in many cases similar to normal polymers. Large parts of the chain are uncharged and the PE structure in solution can be correlated to the solvent quality [2, 55]. The only difference between polymers and PEs is the additional contribution of the electrostatic charges. Therefore, it is not surprising that some of the first and, until now, most frequently used thermodynamic approaches were mean field and Flory based [1, 2, 16]. A convenient way to take the charged groups into account is by considering the electrostatical repulsion of the monomers and multiplying it by the fraction of charged groups, f. The free electrostatic energy of a PE is therefore dependent on the dielectric media and fraction of charged monomers [2, 16]:

$$F_{el}(R) \approx k_B T \frac{l_B (fN)^2}{R} \ln\left(\frac{R}{bN^{0.5}}\right) \tag{21}$$

It is worth noting that, depending on the type of PE used, the electrostatic contribution for PEs are the dominating force and therefore it is possible to omit the Flory enthalpy term in this cases [23]. If the PE is very weak, the free enthalpy of dilution, ΔH, is only correctly obtained, when the electrostatic and Flory-Huggins polymer dilution enthalpy terms are added [49].

$$\Delta H_{dil} = \Delta H_{Flory} + \Delta H_{el} \tag{22}$$

$$\Delta F_{Flory} = \chi R T \upsilon_2 \tag{23}$$

where χ is the Flory-Huggins solution parameter [44]. ΔH_{el} is calculated from the difference of the total electrostatic energy, H_{tot}, before $_{(b)}$ and after $_{(a)}$ dissolving or diluting the PE [49].

$$\Delta H_{el} = H_{tot(b)} - H_{tot(a)} \tag{24}$$

H_{tot} consists out of 3 parts, namely E_D, which is the Debye electrostatic energy of the PE chain, E_a, the energy of the counterion adsorbed on the PE, and E_{ela}, the elastic energy of the stretched, or charged PE [49]. These parameters are defined according to Safranov [49] with the fraction of free counterions, β, as:

$$E_a = \frac{e^2 N_a}{b\varepsilon}(1-\beta^2)\ln \upsilon_2 \tag{25}$$

$$E_D = -\frac{e^2 N_a}{b}\left(\frac{\beta}{\varepsilon}\right)^{3/2}\sqrt{Au\upsilon_2} \tag{26}$$

$$E_{ela} = \frac{e^2 N_a}{b}\left(\frac{b}{a}\right)^{5/7}\left(\frac{\beta}{\varepsilon}\right)^{10/7} u^{-2/7} \tag{27}$$

where the constant $A = \sqrt{8\pi}$, and the charge density parameter, u, is defined as [49]:

$$u = \frac{e^2}{\varepsilon k_B T b} \tag{28}$$

The PE total electrostatic based energy for 1 mol of monomer units is therefore a sum of (25–27) [49]:

$$E_{tot} = \frac{e^2 N_a}{b}\left[(1-\beta^2)\ln \upsilon_2 - \left(\frac{\beta}{\varepsilon}\right)^{3/2}\sqrt{Au\upsilon_2} + \left(\frac{b}{a}\right)^{5/7}\left(\frac{\beta}{\varepsilon}\right)^{10/7} u^{-2/7}\right] \tag{29}$$

Equation (29) was investigated with high molecular weight chitosan (MW $\sim$ 20,000 g/mol) [49]. A partial alkylation of the chitosan monomer groups allowed the authors to verify Eq. (29) for different degrees of electrostatic and apolar interactions between PEs and PE with water [49].

Poly(L-glutamic acid) displays a different behavior compared to other weak PEs [56], showing a strong dependence on the degree of polymerization [57]. One of the reasons for such a behavior is the big difference in structure between natural and synthetic polymers e.g. synthetic polymers are coiled, while poly(L-glutamic acid) has a helix like conformation in a low charged state [57]. For such a poly (L-glutamic acid) like system the electrostatic enthalpy dominates [57]. The electrostatic enthalpy of dissolution can be calculated with the semi-empirical formula from Scerjanc [56] who developed his formula originally for a polyacrylic acid system [57]:

$$\begin{aligned} H_e = &\frac{fnRT}{n\lambda}\left[(1-k_1)k_2 - \ln\left(\frac{(1-\lambda)^2-\beta^2}{1-\beta^2}\right) - \lambda\right]\left(1 + \frac{T}{\varepsilon} - \frac{\Delta\varepsilon}{\Delta T}\right) \\ &+ \frac{fnRT}{2n\lambda}\left(1 - \beta^2 - \frac{\lambda z_e^{2k_2}}{z_e^{2k_2}-1}\right)\left(\frac{\Delta \ln V}{\Delta \ln T} + \frac{\Delta \ln R}{\Delta \ln T}\right) \end{aligned} \tag{30}$$

In (30), k_1 is a constant related to λ, and the concentration parameter, k_2, which is proportional to $-\log c_P$. In (30) z_e is the Euler number; n is in this case the valence of the monomer group. V is the volume of the solution and the charge density parameter, λ, is defined as [56]:

$$\lambda = \frac{enfe_0^2}{\varepsilon a k_B T} \tag{31}$$

where a is defined as the monomer length. ΔH of dilution is calculated in the same way as in Eq. (24) [56]. Equation (30) is based on the model of Katchalsky and Kuhn [2], and is not applicable for low degrees of ionization since in such a case non electrostatic interactions become dominant [56, 58]. In this case use of

Eq. (22–29) is suggested. The formulas (22–30) are all normalized for 1 mol of monomer units. Another method is to use the novel method of Muthukumar [59] which allows also the adjustment of the fraction of charged monomers—see formulae in the strong PE section (43–47).

For enthalpy driven PE complex formation and other processes in weak PEs, see Sect. 3.3.

3.2.2 Strong Polyelectrolytes

In the case of strong PEs, the properties of the PE, and therefore of the enthalpy, are mainly controlled by the strong electrostatic coupling (see above). Therefore the Debye-Hückel approach is more frequently used than in case of weak PEs. The enthalpy upon dilution of the PE is mainly influenced by the dissociation of the PE and the counterions [15]. The free electrical energy of the PE upon dilution is, according to Osawa [15]:

$$\frac{E_e}{k_B T} = \frac{1}{2}\frac{e_0^2}{k_B T a} n^{*2} N_M \tag{32}$$

Here n^* is the number of charged groups in the PE. The free energy of the electrolyte part of the PE is, therefore:

$$\frac{F_e}{k_B T} = \frac{E_e - T S_e}{k_B T} \tag{33}$$

where the entropy of the electrolyte part, S_e, is discussed in detail in Sect. 3.4. The total free energy is, according to Osawa, therefore a combination of the free energy of the electrolyte, the mixing entropy, S_M, the Kuhn entropy S_K (which is related to the PE structure) and the contribution of the ion atmosphere, F_A, which is, however, small compared to F_e [15]:

$$F = F_e + F_A - T(S_M + S_K) \tag{34}$$

Since the early approaches which led to the equations presented in references [2, 58] showed a unreliable correlation between the molecular size and the free electrical energy, empirical formulae with free variables were established [60]. These empirical functions are based on an assumption similar to Eq. (34) and can be found in Ref. [15].

A successful theoretical solution to the problem by means of statistical thermodynamics was first achieved by Mandel [61]. This solution was later extended significantly by Manning [3]. The limits of this approach, which is unable to predict the helix to coil transition of DNA and sometimes delivers results one order of magnitude too high, were also pointed out by Manning [3]. The counter ion condensation leading to the famous Manning-Osawa counterion condensation

theory was the focus of Manning's study. Despite the Manning-Osawa theory of counter ion condensation bearing the name of both, the function for the free energy of PE dilution, obtained by Manning, and which incorporates the possibility of multivalent ions [3], is quite different from that of Osawa which is only valid for monovalent ions [compare (35) with (32)].

$$F_{mix} = \theta_n \ln\left(\frac{10^3 \theta_n V_1^{-1}}{c_S}\right) \tag{35}$$

where θ_n is the fraction of associated counterions per monomer and all counter ions have the valence n. θ_n is defined as $\frac{q_{net}}{q} = 1 - N\theta_n$ [3]. The PEs can adopt various structures in solution, such as a coil or helix [3]. To adopt these structures, the free energy of the structural change must be larger than the electrostatic repulsion which is [3]:

$$F_{el} = (1 - N\theta_n)^2 \zeta \ln(1 - e^{kb}) \tag{36}$$

The minimum free energy needed to cause a change in molecular structure for highly diluted solutions ($c_P \to 0$), where $\theta_n \approx \zeta$ is [3]:

$$\Delta(F_e - F_0) = \Delta(1 - \zeta^{-1}) \ln\left(\frac{c_I^{loc}}{c_I}\right) - \zeta^{-1} \ln(kb) \tag{37}$$

Here, F_0 is the non electrostatic contribution to the free energy. An interesting comparison done by Manning was the comparison of the bending capability of the PE with the persistence length. Although this estimate of the free energy does not contain the entropic contribution, it allows an interesting estimate of the change in electrostatic energy with changes of the persistence length (38) [3].

$$\Delta F = \frac{(RTa)}{2l_P} \theta_n^2 \tag{38}$$

The resulting free energy for a spontaneous structure change from straight to bent is therefore [3]:

$$\Delta F = \Delta F_0 + \left(\frac{\theta^2}{24}\right) \zeta^{-1} \left[2\zeta - 1\left(\frac{c_I^{loc}}{c_I}\right) \ln(kb)\right] \tag{39}$$

Michaeli and Overbeek used the Debye-Hückel approach to estimate the enthalpy of the PE–PE and PE-solvent interaction [23]. In this model, the Flory entropy is used as the entropic term of the PE chain, and the electrostatic free enthalpy is calculated from the electrostatic energy of a strong PE [23]. By thermodynamic considerations, Michaeli and Overbeek showed that for small univalent counterions no coacervation (complex-formation between PE) occurs

because the entropy of counterions outbalances the enthalpy (see Sect. 3.4), favoring coacervation [23]. This finding was true for two approaches which were compared by Michaeli and Overbeek, one was the Debye-Hückel theory (40) and the second from Lifson and Katchalsky (41) [23]:

$$\frac{G_e}{V} = \frac{k^3 k_B T}{12\pi} = B\left(\sum_j n_j^* v_j\right)^{3/2} \varepsilon^{3/2} T^{1/2} \tag{40}$$

with j being the type of molecule carrying the charge, $B = 2/3\pi^{1/2} k_B^{-1/2} e^3$ and e_e the electron charge.

$$G_e = N_M F_e \text{ and } \bar{G}_e = \frac{v_1}{v_P} F_e \tag{41}$$

Both methods showed that the PE coacervation depends on the PE concentration and on the type and concentration of counterions [23]. Equation (41) is especially tempting to use due to its simplicity. However, since the approach is limited to low concentrations, its applicability for most flexible synthetic polymers at high concentrations is very limited [58]. In contrast, for rod-like, rigid polymers like Tobacco mosaic virus which can not change its shape, it can also be used for higher concentrations [58]. Equation (40) was extended in a subsequent paper by Overbeek for cases where the PE and the counterions are not equal and a second solvent with a low dielectric constant has been added [62].

An interesting novel way to determine the Gibbs free enthalpy of PE-salt complexes within PEM thin films exposed to salt solutions is via the reaction constant [63]:

$$\Delta G_{assoc} = RT \ln K_{assoc} \tag{42}$$

Here K_{assoc} is the association constant. To utilize this method, one must do either an isothermal titration or measure a series of changes in IR-spectra to determine the association constant [63]. It is worth noting that the degree of ion doping and water incorporation correlates with the Hofmeister series [63]. Since PE–PE bonds are broken by incorporation of counter ions, the association constant can also be used indirectly to estimate the PE–PE interaction strength. Calorimetric measurements done by Schlenoff to directly determine the enthalpy of PE complex formation for strong PEs, resulted in values close to 0 [63].

Theoretical determinations of the counterion distribution around a PE were done by Solms by approximating them as tangentially bonded spheres which interact via the coulomb potential [64]. In his work, the Osmotic pressure and thermodynamic properties were determined via analytical integrals [64].

One interesting contribution to the study of PEs was done my Muthukumar [59]. In his extended theory of the counterion condensation of Manning, six contributions to the free energy are considered [59]:

$$F = F_1 + F_2 + F_3 + F_4 + F_5 + F_6 \tag{43}$$

where F_1 is the entropy of the condensed counterions, F_2 is the translational entropy of condensed and free ions (except the PE), F_3 represents fluctuations between the dissociated ions (without PE), F_4 is the gain in energy due to counterion adsorption (ion pair formation), F_5 is the free energy of the PE with its degree of dissociated monomers, and F_6 includes the correlations between ions pairs and the PE. For the entropic contributions (F_{1-3}) of Muthukumar's theory, see Sect. 3.4.2 formulas (56–58). F_4 is defined as the contribution of the ion pair energy to the free energy, with the energy of one ion pair being $-e^2/(\varepsilon_0 \varepsilon_l \pi l_d)$ [59]:

$$\frac{F_4}{N_C k_B T} = -(1-f)\left(\frac{\varepsilon}{\varepsilon_l}\right)\left(\frac{l_M}{l_d}\right)\left(\frac{l_B}{l_M}\right) \tag{44}$$

Here, ε_l is the local dielectric constant, l_M is the length between two monomers, and l_d is the length of the dipole and N_C is the number of counter ions. F_5 depends on the electrostatic repulsion energy and contains the expansion factor $Z_1 = 6R_G/(l_M^2 N_C)$ [59]:

$$\frac{F_5}{k_B T} = \frac{3}{2}(Z_1 - 1 - \log Z_1) + \frac{4}{3}\left(\frac{3}{2\pi}\right)^{3/2} W\sqrt{N_C}\frac{1}{Z_1^{3/2}} + 2\sqrt{\frac{6}{\pi}} f^2 \tilde{l}_B \frac{N^{3/2}}{Z_1^{1/2}}\Theta_0 \tag{45}$$

R_G is the radius of gyration, W a strength parameter for short ranged effects and Θ_0 and Z_2 are:

$$\begin{aligned}
\Theta_0 &= \frac{\sqrt{\pi}}{2}\left(\frac{2}{Z_2^{5/2}} - \frac{1}{Z_2^{3/2}}\right)\exp(Z_2)erfc(\sqrt{Z_2}) + \frac{1}{3Z_2} + \frac{2}{Z_2^2} - \frac{\sqrt{\pi}}{Z_2^{5/2}} - \frac{\sqrt{\pi}}{2Z_2^{3/2}} \\
Z_2 &= \frac{N_C Z_1 \tilde{\kappa}^2}{6} \\
\tilde{\kappa}^2 &= \tilde{l}_B 4\pi(f\rho l_3^3 + 2c_S l_M^3)
\end{aligned} \tag{46}$$

Since several parameters needed to be correlated with the local volume, κ became $\tilde{\kappa} = \kappa l_M$ and the density and salt concentration parameter were multiplied by the monomer volume. The correlation between the ion pairs and the PE are defined as [59]:

$$\frac{F_6}{k_B T} = \frac{4}{3}\left(\frac{3}{2\pi}\right)^{3/2} Z_2 \left(\left(\frac{\varepsilon}{\varepsilon_L}\right)\left(\frac{l_M}{l_d}\right)\right)^2 \tilde{l}_B^2 \left(\frac{l_d}{l_M}\right)^6 (1-f)^2 \sqrt{N_C}\frac{1}{Z_1^{3/2}} \tag{47}$$

This theory allows the PE to bent due to entropy, including at low ionic strength, and allows PE of a finite length, in contrast of Mannings theory. For an alternative definition of F_6 and its derivation, see Ref. [59].

Complex formation of strong PEs is mostly dependent on the entropy. The enthalpy changes of nearly all processes and complexes of strong PEs are 2–15 times smaller than the changes in entropy. For details of the entropy see Sect. 3.4 [63, 65]. The enthalpy of complex formation can be calculated with the formalism of Overbeek (Eq. 40–41) [62], or with the method of Muthukumar (43–47) [19, 59]. Another method is to determine the enthalpy of complex formation by isothermal calorimetric titrations or other calorimetric methods, turbidity titrations or molecular dynamics simulations [19, 63, 65]. Recent molecular dynamics simulations [19] and experimental measurements showed that the enthalpy of PE complex formation decreases with increasing ionic strength, but this value is always below the entropy [23, 62, 63, 65]—see following section for detail.

3.3 Enthalpy-Driven Processes in Weak Polyelectrolytes and Polyelectrolyte Complexes

The behavior of weak PEs is mostly controlled by the pH and ionic strength. If e.g. the pH causes a very low charge density, the interaction between the PEs and also within the same coil is controlled by hydrophobic forces and hydrogen bonds [65]. An interesting finding is that the process of complex formation of two oppositely charged weak PEs is only enthalpy controlled when the PEs are in a region of a low charge [66]. At low or intermediate charge, when the PE is able to form hydrogen bonds, the enthalpy of a weak PE is ~ 3 times the enthalpy of a strong PE [66]. The complex formation can be switched to an endothermic process for conditions where the PE is strongly charged (e.g. change of pH) and then the process is entropy controlled like in the case of strong PEs [66, 67]. The ratio of the PE charge types within the PE–PE complex formed (e.g. positively to negatively charged ratio, with charge neutrality caused by small counter ions) can also be triggered by the pH value [65, 68–71]. The addition of a solvent with a low dielectric constant can decrease the free enthalpy as well [65]. The enthalpy can, if the PE is controlled to a large extent by electrostatic forces, be calculated via the formulas of Overbeek [23]. Equations (40–41) or from Manning [3] (37–39). Despite the formulae being developed for strong PEs, they have been proven to be adequate for weak PEs as well. A special formula for very low charge density or hydrogen bond dominated PE interactions has, to the knowledge of the author, not yet been established. A possible reason for the lack of such a formula might be the large diversity [65] of available weak PEs and the complex interplay between the forces.

One of the main interactions in weak PEs that contribute to the enthalpy are hydrogen bonds, which allow the e.g. natural PE to adopt special structures, like helices [3, 57]. The fact that the initial structure of a weak PE (coil or helix)

influences the stoichiometry of the complex formation further increases the difficulty of establishing a mathematical formalism [72]. In the case of proteins, which are natural PEs, the structure as well as aggregation behavior is often more complex, which has lead to high computational efforts [73]. Due to these high computational efforts [66], measurement based values like direct measurement from the isothermal calorimetric titration [66], crystallography, or from measured reaction constants like in Eq. (42) [63] seem more feasible.

It is to be expected that, in the near future, an extension of novel theories like those of Muthukumar [19, 36, 59] or the 0th order Gaussian equivalent renormalization theory (GER0) from Baeurle [74] will solve some of the afore mentioned problems for the computation of weak PEs. The group of Baeurle solved the problem that long equilibration times, low temperatures and increasing complexity of polymers caused a decreasing efficiency of grand canonical functions by integrating a Monte Carlo Auxiliary field into the grand canonical function at high polymer densities [74, 75]. Especially the GER0 approach solves many problems that emerged in the field theoretical modeling of PEs and has already successfully been used to determine the osmotic pressure of weak PE solution in various concentration regimes [76, 77]. It is, however, already clear that not one function alone will solve all the issues with this type of PE. In particular, since MD functions are too computationally expensive and the observable timescales too short, and the GER0 formalism is not usable for single or polymer nano-structures [78, 79]. For complexes of biological PE, recently a mixture of kinetic Monte-Carlo and Molecular dynamics approaches was used to determine the signaling pathway of proteins [78]. For nanostructures of block copolymers, the same group recently used a self-consistent field method [79]. This will allow a simplified computation of the enthalpy and entropy of complexation and non-coiling structures of synthetic, weak PEs, and some natural ones with simple structure.

3.4 Entropy in Polyelectrolyte Solutions

3.4.1 Weak Polyelectrolytes

In the case of weak PEs, the PE remains stiff and rod like if the PE blob size is small compared to the chain length [22, 29]. Therefore the change in entropy upon dilution or complex formation [21] of such a PE is small. In the case of a weakly charged PE, where the electrostatic repulsion is smaller than k_BT, a Gaussian coil like conformation of the PE emerges within afore mentioned blob sizes. The entropic structure of the PE within blobs is the same as in the case of uncharged polymers. Considering both enthalpy and entropy in a Flory-like mean field system to describe the solution behavior of a weak PE, taking the polymerization degree, N, the charged fraction, f, the length of the (coiled or elongated) PE, L, the Bjerrum length, l_B and the thickness of the PE (partially coiled), $b\sqrt{N}$, leads to the approach of Kuhn [2]. The free energy of a PE in solution is therefore [2, 26]:

$$F \approx \frac{L^2}{b^2 N} k_B T + k_B T \frac{l_B (fN)^2}{L} \ln\left(\frac{L}{b\sqrt{N}}\right) \tag{48}$$

The first term of (48) is the contribution of the chain conformation to the free energy and it is inversely related to the entropy. If the entropy decreases (e.g. the chain gets elongated), L increases, and the first term on the right hand side of (48) will increase as well. The second term of (48) represents the electrostatic contribution of the PE to the free energy. Equation (48) is therefore able to determine the overall structure of a PE depending on the fraction of charged monomers. This allowed Kuhn to calculate and evaluate the degree coiling of the PE depending on the charged fraction, as well as to predict the viscosity from the structure of the PE and to compare it with measurements of the viscosity of the corresponding solutions [2].

Since viscosity measurements of uncharged, weak and strong PEs [60] were successfully modeled with the Kuhn entropy [80], it should theoretically be possible to describe weak PE solutions with it as well. This assumption is supported by the fact that the Kuhn entropy is based on the Boltzmann entropy formula, and attempts to use this approach become inaccurate to determine the ion distribution around the charged groups of strong PEs at low salt concentrations, but not the PE structure [81]. Since weak PEs are not strongly affected by counter ion condensation, these effects pose no problem for the Kuhn entropy approach. Another reason for the infrequent use of the Kuhn entropy is the fact that the Flory approach is much simpler and better known than the Kuhn approach [49, 80, 82].

The original theoretical assumption that the low charge density has a negligible influence on the structure is supported by experimental measurements of Safronov et al. [49]. Their results showed no influence from salt concentration, and therefore of the charge density, on the dilution enthalpy or total energy of chitosan, (a weak PE) [49].

3.4.2 Strong Polyelectrolytes

Strong PEs show a fundamentally different dilution and complex formation behavior compared to weak PEs. Dilution is mainly driven by the increase in entropy from the release of counterions and not, like in case of weak PEs, by changes of the enthalpy [15, 62]. The structure of the PE itself, as well as its enthalpy, changes only a little during these processes [63, 65]. The change in the counterion and other ion entropy was calculated by Osawa to be:

$$\begin{aligned} -\frac{S_e}{k_B} = &-\frac{e_e^2}{\varepsilon k_B T a_1} n^{*2} N_C + N N_C \ln \frac{N}{N_{1i}} \frac{1+\sqrt{1+\delta^2}}{2} \\ &+ c_S \ln \frac{[c_S (N - n_+) N_C][c_S - n_- N_C]}{N_{1O}^2} + N N_C + 2 c_S \end{aligned} \tag{49}$$

$$a_1 = n_+^{1/3} 8A \tag{50}$$

$$\delta^2 = \frac{v_0^2}{N^2} \frac{c_S}{V_-} \frac{NN_C + c_S}{V_+} \tag{51}$$

where A represents the unit Å, V_- and V_+ are normalization factors obtained by integrating over the π bonds [15]. The free electric energy of the system is therefore dependent on the entropy of the counter ions and the electrostatic energy of the PE, as shown in Eq. (33) [15]. The function of the total entropy can be found in Eq. (34), where the terms for the entropy of mixing can be approximated by the ideal entropy of mixing at very low PE concentrations. The Kuhn entropy, which adds to the mixing entropy, depends on the size and shape of the PE and emerges due to microbrownian motion. The Kuhn entropy for the PE chain was used by Kagawa et al. [60] in their paper to determine the free energy of strong PEs by means of statistical thermodynamics. The Flory approach combined with a random phase approximation was successfully used in other studies [82, 83] to determine the gelation threshold at high concentrations of strong PEs in presence of multivalent counterions. Another method also applied to strong PEs is just to use the Flory entropy stated in Eq. (19) [23].

A very simple term for estimating the change in entropy of the counterions upon dilution was used by Manning. Since the association of the counter ions depends on the concentration of added salt, the entropy of the conuterions scales inversely to the salt concentration [3]:

$$S_e \sim nR_G \ln\left(\frac{c_S^{loc}}{c_S}\right) \tag{52}$$

The relation (52) is part of Eqs. (37) and (39).

A volume fraction based term for the determination of the entropic contribution of the (small) counter ions was utilized by Overbeek and Michaeli [23].

$$S_C = \frac{v_1}{v_l} k_B T \ln v_1 + \frac{v_3}{v_C} k_B T \ln v_3 \tag{53}$$

The entropy of the PE chain consists of terms based on volume fractions for the PE and solvent and additionally the ionic species, i, in a Flory-Huggins like expression. For this reason Eq. (49) is more general than Eq. (48) [23].

$$S_{mix} = \frac{k_B T}{v_l} \left(v_1 \ln v_1 + \sum_i \frac{v_i}{r_i} \ln v_i \right) \tag{54}$$

Please note that Eq. (54) is very similar to recent theories and computer simulations based on molecular dynamics [19]. The free enthalpy is therefore [23]:

$$G = G_e + S_{mix} \tag{55}$$

Since the change in molecular entropy of the PE chain itself is often small, compared to the entropy of the counter ions, S_{mix} can often be replaced with the entropy of the counterions S_C. G_e in Eq. (55) can be found in Eqs. (40–41).

The cell model from Katchalsky, Onsager and Manning, which was originally only applicable to linear PEs [26], was extended by Deshkovski in 2001 to a more general two zone model based on the mean field approximation of the nonlinear Poisson Boltzmann equation [84]. In this two zone model, the counter ions around a cylindrical rod (PE) form the area close to the PE, and a spherical volume which extends up to the distances between the PE is the area far away from the PE [84]. This model is able to explain the mean distance of the counterions from the PE chain as a function of the counterion concentration.

The most detailed entropic consideration until now is used by the formalism of Muthukumar. In this formalism, three different entropic contributions to the free energy, which consists of a total of 6 contributions [see Eqs. (43–47)], are considered. The entropies are [59]:

$$\frac{F_1}{N_C k_B T} = f \log f + (1-f)\log(1-f) \tag{56}$$

$$\frac{F_2}{V_l k_B T} = (fc_P)\log(fc_P + c_S) + c_S \log c_S - (fc_P + 2c_S) \tag{57}$$

$$\frac{F_3}{V_l k_B T} = -\frac{1}{3}\sqrt{4\pi} l_B^{3/2} (fc_P + 2c_S)^{3/2} \tag{58}$$

In (56–58) the entropy of the condensed counterions are defined by F_1; the translational entropy of the ions is F_2; and the fluctuations between PE and ions is given by F_3. Another way to determine the entropy of the PE solution or complexes is by e.g. isothermal calorimetry measurements with simultaneous determination of the reaction constant [63].

3.5 Entropy-Driven Processes in Strong Polyelectrolytes

In case of strong polyelectrolytes, the complex formation, as well as dilution in a solvent, is driven by counterion release [15, 23, 58, 63]. The reason for the strong dominance of the entropy is the fact that there is only a little change in the

enthalpy of the PE in solid, solution or the complex, in comparison to the entropy of the counter ions [15, 23, 60, 62]. Therefore the entropy outweighs the enthalpy in the described processes by a factor of two to fifteen [63]. As already reported in the 1950s, the PE will not form complexes or phase separations in water with only monovalent counterions at low or moderate concentrations due to the strong contributions of the entropy [23].

One way to increase the electrostatic interaction energy, and at the same time to decrease the entropy, is to exchange the monovalent counterions with multivalent ions or oppositely charged PEs [23]. This way one can achieve concentration dependent complex formation, or coacervation, within the PE solution. At low concentrations, the PE-counterion complex, whereby the counterion is a polymer or multivalent salt, will be strongly charged. The addition of salt to the solution shields the PE charge and decreases the PE–PE or PE-multivalent ion tendency to phase separate due to shielding of the charges [23]. Such a behavior was indeed measured with the dissolution of PE multilayer thin films (two dimensional thin films comprising of complexes of oppositely charged PE) in high ionic strength solutions [85], as long as the PE did not salt out. Figure 2 illustrates this effect, by showing the range of solubility for two PEs of the same size and charge density with opposite charges at different salt and polymer concentrations. It can be clearly seen that high salt concentrations at moderate PE concentrations cause a high solubility (point C in Fig. 3).

3.6 Viscosity of Polyelectrolyte Solutions

To understand the rheological and viscous behavior or PE solutions it is vital to understand the behavior of PE molecular structure, entanglement and interactions in solution. This is because the PE viscosity behavior is dominated by the PE structure, giving PE solutions unique properties compared to uncharged polymers [26, 86]. Another contribution to the solution viscosity is the viscosity of the solvent, η_s, and the interaction of the solvent with the polymer or polyelectrolyte, which is important since the PE will always drag some solvent molecules with it upon movement and shear force [2, 80, 87, 88]. The scaling laws of solution and PE structure in relation to viscosity were mainly developed by de Gennes and Pincus with contributions to the entangled regime by Pfeuty [22, 53, 89]. The friction coefficient of a colloidal particle (here a spherically coiled PE) used in the scaling theory in solution can be determined by the Stokes law [30]:

$$Z_P = 6\pi\eta R \tag{59}$$

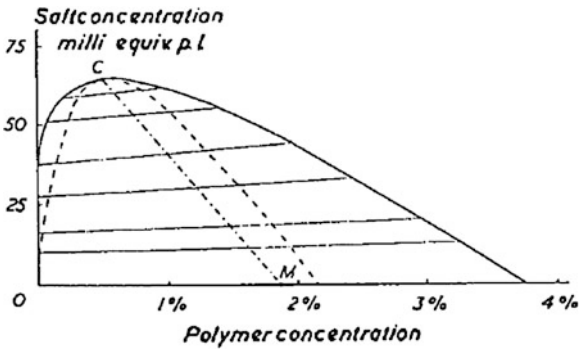

Fig. 3 Addition of a large amount of salt increases solubility of PE and lowers complex formation. The area below the *curve* is the dissolved region, where the *dashed line* shows the spinodial and the line C-M the rectilinear diameter. Image taken from Ref. [23], reprinted with permission of John Wiley and Sons

Here η is the viscosity, which is the proportionality coefficient of the shear, rate $\dot{\gamma}$, and the shear stress, σ_s [30].

$$\eta = \frac{\sigma_s}{\dot{\gamma}} \tag{60}$$

The diffusion coefficient of a spherical particle in a liquid is defined by the Stokes-Einstein relation [30]:

$$D_i = \frac{k_B T}{6\pi\eta R} \tag{61}$$

Equation (61) is especially important because many measurement systems like dynamic light scattering or pulsed field gradient NMR do not measure the absolute diffusion and viscosity, but the relation to the hydrodynamic radius. The hydrodynamic radius, R_H, is defined as [30]:

$$R_H = \frac{k_B T}{6\pi\eta D_i} \tag{62}$$

The volume fraction, ϕ, is calculated from the concentration, the molar mass of the monomer, M_{Mon}, the density ρ and the monomer volume. The Avogadro constant is N_{av} [30].

$$\phi = \frac{c}{\rho} = \frac{c}{M_{Mon}} b^3 N_{av} \tag{63}$$

The time, τ, a polymer or bead needs to travel a distance on the order of its own size is dependent on the friction coefficient, Z_P [30].

$$\tau \approx \frac{R^2}{D_i} \approx \frac{R^2 Z_P}{k_B T} \tag{64}$$

The inverse dependence of τ on the temperature is caused by the fact that the PE travels due to diffusion. The random collisions of the solvent molecules on the PE coil cause an increased diffusion speed with increasing temperature due to introduction of more kinetic energy.

There are two theoretical models to determine the relaxation time, τ_R, and self-diffusion time of the PE in the solution. One is the Rouse model, which is based on the assumption that the PEs are comprised of mass centered points connected with springs these points only interact with these springs. The other is the Zimm model which is an extension of the Rouse model and takes hydrodynamic effects into account [24, 30]. The Rouse model was used to establish the scaling theory of PEs in solution, which allows an estimation of the PE structure from the viscosity in the different solution regimes.

Before the current state of the art of the scaling regimes of viscosity values for PE solutions in different concentration regimes is introduced, it is worth noting, that it can still not explain all observed effects. The calculated values still deviate from measurements, especially at the transition points between concentration regimes. The same is true for osmotic measurements. Novel theories like the GER0 theory can explain all concentration regimes, from dilute to entangled concentrations, while showing a smooth transition. However only the scaling regimes for the osmotic pressure were calculated and tested by the authors [77]. It is expected, that an application of the GER0 theory in the field of rheology in the near future will solve the remaining theoretical gaps.

3.6.1 Unentangled Dilute Regime

The relaxation times determined by the Rouse model, τ_{RR}, and diffusion coefficient, D_R, in the unentangled regime (very low concentration without chain-chain interactions) is [24, 26]:

$$\tau_{RR} = \frac{\eta_S b^3 N^2}{k_B T} \tag{65}$$

The concentration dependent relaxation time of the p modes (p = 1, 2, …N) [30]:

$$\tau_P \approx \tau_0 \left(\frac{N}{p}\right)^2 \tag{66}$$

The mode p = 1 is the longest relaxation mode and is τ_{RR}. For the modulus of the Rouse model, see Ref. [30]. The rouse diffusion constant is defined as [30]:

$$D_R = \frac{k_B T}{N Z_P} \tag{67}$$

The viscosity contribution of the PE to the solution viscosity is defined as [30]:

$$\eta - \eta_S \approx \frac{Z_P}{b} \phi N \tag{68}$$

In contrast to the Rouse model, the Zimm model on the contrary is more precise for low concentrations since the Rouse model is only precise in polymer melts, ignores solvent effects and applies precisely only at high PE concentrations [30]. A comparison of the relaxation times from the Rouse and Zimm models was done in Ref. [30]. For the case when the correlation length is smaller than the screening length (strong dilution), the Zimm time is usually shorter than the Rouse time. This surprising result was explained with the springs in the Rouse model, which hinder free motion of the mass centers. In contrast, a PE in the Zimm model can freely diffuse within the solvent or take part in a mixed motion including additional diffusion of monomers in the chain [30]. The relaxation time and diffusion of the Zimm model, τ_{RZ} and D_Z respectively, in the unentangled regime of an ideal chain are, according to [30].

$$\tau_{RZ} = \frac{1}{2\sqrt{3\pi}} \frac{\eta_S}{k_B T} R^3 \tag{69}$$

$$D_Z = \frac{8}{3\sqrt{6\pi^3}} \frac{k_B T}{\eta_S R} \tag{70}$$

The concentration dependent viscosity of the Zimm model is defined as:

$$\eta - \eta_S \approx \eta_S \phi N^{3\nu - 1} \tag{71}$$

where ν is ~ 0.5 in θ solvents and ~ 0.666 in good solvents for PEs. This value for good solvents is strikingly different from the ones of uncharged polymers which is ~ 0.588 in good solvents. These differences are caused by charges with the same sign in the PE repelling each other, leading to a final scaling exponent of 1 $(3 \cdot 0.666 - 1 = 1)$ [30]. In case of weakly or partially charged PEs, the overlap concentration, c*, is changed but not the exponent of the PE solution regime [26]. As can be seen in above equations, the contribution of the PE to the solution viscosity is linear at concentrations below c*. For a comprehensive explanation of the Zimm modes and relaxation time, see Ref. [30].

3.6.2 Unentangle Semidilute Regime

In case of semidilute systems without entanglement (c > c*), in regions above the correlation length, the Rouse motion is faster than the Zimm motion because the Zimm motion is hindered by a coupling between the chains and Rouse dynamics apply [30]. For a detailed derivation of the Rouse and Zimm models, the scaling theory and some older viscosity reviews see references [24, 30, 90].

In the semidiluted unentangled concentration regime the polymer chains begin to overlap but are not entangled. The correlation length decreases with increasing concentration, which agrees with the Fuoss law [17, 24]:

$$\phi \approx \frac{gb^3}{L_\xi^3} \tag{72}$$

With L_ξ being the correlation length which is, in semidilute solutions, equal to the screening length [26, 30]. As can be seen in Eq. (72) the correlation length decreases with increasing concentration, where the size of the chain correlates with the concentration $(L \sim c^{-1/4})$ in a slightly smaller ratio than the distance of the mass centers $(L_M \sim c^{-1/3})$ [26]. This effect allows the unentangled semidilute regime to span over 3–4 decades of the relative entanglement concentration space (c_E/c^*). The correlation of the scaling of the correlation length to the concentration is defined as [30]:

$$L_\xi \approx b\phi^{-\nu/(3\nu-1)} \tag{73}$$

ν has the values mentioned for Eq. (71): ½ for θ solvents and 0.76 for good solvents. The relaxation time of a chain, τ_{chain}, is therefore [30]:

$$\tau_{chain} \approx \frac{b^3\eta_S}{k_BT} N^2 \phi^{(2-3\nu)/(3\nu-1)} \tag{74}$$

The diffusion constant in the semidiluted unentangled regime as a function of the concentration can be calculated from the relaxation time (74) and the size of the polymer [30]:

$$D \approx \frac{R^2}{\tau_{chain}} \approx \frac{k_BT}{\eta_S b} \frac{\phi^{-(1-\nu)/(3\nu-1)}}{N} \tag{75}$$

The concentration dependent viscosity is defined as [30]:

$$\eta - \eta_S \approx \eta_S N \phi^{1/(3\nu-1)} \tag{76}$$

The result of relation (76) is the concentration dependent viscosity in good solvents increases by an exponent of 1.28, while a value of 0.5 causes an exponent of 2. The values 0.76 and 0.5 are for neutral polymers which show no concentration

depended decrease in chain length like PEs. Therefore the value for v in Eq. (76) is ~ 1 leading to a total exponent of 0.5. A correlation of the viscosity which also takes the charge density of the PE into account was suggested by Dobrynin and Rubinstein to be [26]:

$$\eta \approx \eta_S (K f_*^2)^{1/2} (b^3 c)^{1/2} N \tag{77}$$

3.6.3 Entangled Regime and Entanglement Criteria

The entangled regime in the semidilute region starts at the entanglement concentration c_E ($c > c_E$ with c_E being higher than the overlap concentration c*). The polymer entanglement criteria is assumed to be the same as in the case of uncharged polymers [91–93]. In this criteria only long lived entanglements are considered real entanglements and not temporary overlaps due to fluctuations [91–93]. The effect of tails and dangling bonds are also not considered in this approach due to mean field like assumptions [91–93]. The reason that the overlap concentration, c*, does not show a significant entanglement effect is due to the fact that PE chain and blob sizes decrease with increasing concentration. Another observation is that a chain needs to overlap with n other chains to have significant topological movement for the friction becoming a significant effect, with n_e being a number between 5 and 10 [24]. The dependence of the degree of entanglements and the concentration can be seen below [24]:

$$c_e \approx \frac{n_e}{L^3} \approx c^* \frac{nL^3(c^*)}{L^3(c_e)} \approx n^4 c^* \tag{78}$$

Please note that Eq. (78) was originally published as an equality sign [24]. Since the same author published the same equation as an approximation sign 10 years later in a review paper [26], the equation is shown as an approximation sign [24, 26]. For known crossover, salt and entanglement concentrations, the degree of entanglement points per chain can be calculated [24].

$$n_e \approx (c_e/c^*)^{1/4} ((1 + 2nc_S/c^*)/(1 + 2nc_S/c_e))^{3/8} \tag{79}$$

It is additionally noted that the polymers need a minimum chain length for significant entanglement, which is on the order of 10,000 kDa. For a detailed calculation method of the entanglement chain length, see Ref. [93]. The viscosity at the entanglement concentration is according to Ref. [24]. $\eta \approx n_e^2 \eta_S \approx 50\eta_S$, which is comparable to the equivalent one for neutral polymers.

The entanglement for the PE is characterized by an imaginary tube diameter, a. The tube itself is considered to surround the PE random walk, and the entanglements are defined by the amounts of other PE laying within the tube volume, a^3.

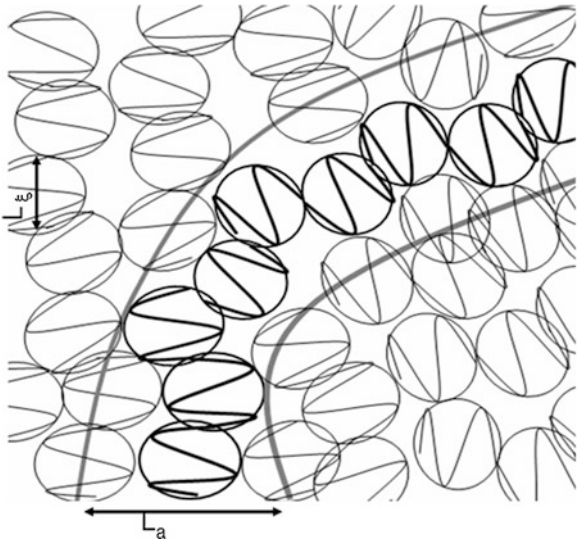

Fig. 4 Definition of the tube diameter, a, also called L_a (length a) and the entanglement criterion of n_E. Image adapted with permission from Ref. [26], copyright of the original version, 2005 Elsevier

Therefore, n_e can be determined by Dobrynin et al. [24] and Dobrynin and Rubinstein [26]:

$$\left(\frac{L_a}{\zeta}\right)^3 \approx \frac{n_e N_E}{N_M} \tag{80}$$

$$n_e = \frac{L_a}{\zeta} \tag{81}$$

The definition of a is shown graphically in Fig. 4.

The longest relaxation time, diffusion constant and viscosity of this region for salt free solutions are according to [24, 26]:

$$\tau \approx \tau_\zeta \left(\frac{N_E}{N_M}\right)^2 \left(\frac{N}{N_E}\right)^3 \approx \frac{\eta_S b^3}{k_B T} K f_*^2 n_E^{-2} N^3 \tag{82}$$

$$D_i \approx \frac{L^2}{\tau} \approx \frac{k_B T}{\eta_S b} n_E^2 N^{-2} (K f_*^2)^{-5/6} (c b^3)^{-1/2} \tag{83}$$

$$\eta \approx \eta_S n_E^{-4} N^3 (K f_*^2)^{3/2} (c b^3)^{3/2} \tag{84}$$

By comparing Eq. (82–84) with each other it can be clearly seen that the parameters are affected in different ways by the concentration. While the relaxation time is only affected indirectly via the amounts of entanglement, the diffusion decreases with increasing concentration by the exponent −1/2, and the viscosity increases by the exponent 3/2. An interesting effect was found for the dependence

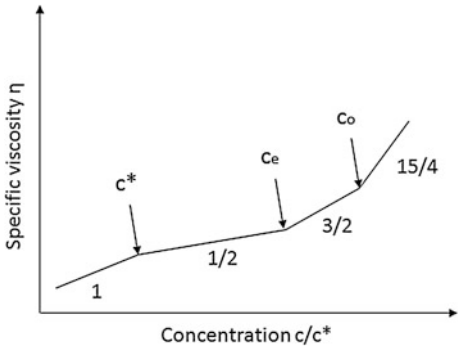

Fig. 5 Illustration of the different concentration regions and their scaling exponent. Image adapted with permission from Ref. [26]. Copyright of the original version 2005, Elsevier

of the viscosity at high salt concentrations. If the concentration of salt is much higher than the PE concentration ($c \ll nc_S$) then the viscosity scales like in the case of neutral polymers in good solvents with $\eta \sim c^{15/4}$ [24]. These regions are illustrated in Fig. 5.

3.6.4 Unentangled and Entangled Hydrophobic Polyelectrolytes in String and Bead Controlled Regions

In case of poor solvents for the PE, like in the case of hydrophobic or partially hydrophobic PEs, formation of necklaces can occur [94]. If the size of the necklace beads reaches the distance between the beads, the PE enters the transition from the diluted to the semidiluted bead controlled regime. The concentration threshold for this regime is defined as [26, 94]:

$$c^* \approx \frac{N}{L_{nec}^3} \approx \frac{N_{Mstr}^{3/2}}{b^3 N^2} \tag{85}$$

An interesting correlation is that the bead size, L_ζ, correlates with the fraction of charged monomers and therefore only weakly and indirectly with the concentration [94].

$$L_\zeta \approx b(Kf^2)^{-1/3} \tag{86}$$

The length of the polymer chain between the beads, called the length of the string, L_{str}, has an inverse correlation with the fraction of charged monomers in the bead [94].

$$L_{str} \approx b(T_R/Kf^2)^{1/2} \tag{87}$$

where T_R is the reduced temperature, $T_R = (\theta - T)/\theta$, with θ being the theta temperature of the PE. In the semidiluted, string controlled, unentangled regime, $c > c^*$, the correlation length can be estimated via following equation [94]:

$$L_\xi \approx R\left(\frac{c^*}{c}\right)^{1/2} \approx b\left(\frac{T_R}{Kf^2}\right)^{1/4}(cb^3)^{1/2} \approx bN_{Mbead}^{1/4}(cb^3)^{-1/2} \tag{88}$$

Here, N_{Mbead} is the amount of molecules in the bead. The concentration at which the bead controlled regime starts can be estimated from either the theta temperature, the charged fraction or from the amount of monomers in the beads [94]:

$$c_b \approx b^{-3}\left(\frac{Kf^2}{T_R}\right)^{1/2} \approx b^{-3}N_{Mbead}^{-1/2} \tag{89}$$

In the bead controlled concentration regime, the correlation length correlates inversely with the concentration, as can be seen in the equation below [94]:

$$L_\xi \approx \left(\frac{T_R}{Kf^2}\right)^{1/3} c^{-1/3} \approx \left(\frac{N_{Mbead}}{c}\right)^{1/3} \tag{90}$$

The overlap concentration of the beads, c_o, is the point at which the concentration of beads reaches values comparable to the PE concentration inside the beads [94]:

$$c_o \approx \frac{N_{Mbead}}{L_\xi^3} \approx \frac{T_R}{b^3} \tag{91}$$

The self-diffusion coefficient in the unentangled string controlled concentration region shows no correlation with the concentration. In the bead controlled region, the diffusion coefficient increases with the concentration. This counterintuitive behavior can be explained with the fact that the friction coefficient is linearly related with the correlation length. Since the correlation length decreases in this concentration regime with increasing concentration, the self-diffusion coefficient increases [94].

$$D_i \approx \frac{k_B T}{\eta_S b}\frac{N_{Mbead}^{1/2}}{N}X \tag{92}$$

Here, X is 1 for the case of $c < c_b$, and $(c/c_b)^{1/3}$ in case of $c_b < c < c_o$.

The relaxation time of the longest mode in the semidilute and bead controlled regime can be determined according to [94]:

$$\tau \approx \frac{\eta_S b^3}{k_B T} \frac{N^2}{N_{Mbead}^{1/2}} X \tag{93}$$

Here, X is $(c_b/c)^{1/2}$ for the case $c < c_b$, and c_b/c in the case of $c_b < c < c_o$. The viscosity also depends on the concentration regimes. In the semidilute regime it scales with the exponent ½, while it is in the bead controlled region independent from the concentration. This phenomena is explained with the inverse correlation of the correlation length to the concentration [94]:

$$\eta \approx \eta_S \frac{N}{N_{Mbead}} X \tag{94}$$

Here, X is $(c/c_b)^{1/2}$for the case of $c < c_b$. and 1 in case of $c_b < c < c_o$.

Entangled necklaces:
The entanglement criterion for necklaces is similar to that for a normal PE. Also, the number of entanglement sites is the same, and the entanglement concentration can be determined by $c_e = n^4 c^*$ [94]. The only difference is the tube diameter and the correlation length defining it. The relaxation time, self-diffusion coefficient and viscosity of entangled PE necklaces can be determined by [94]:

$$\tau \approx \frac{\eta_S N^3 b^3}{k_B T n_e^2 N_{Mbead}^{3/2}} X \tag{95}$$

Here, X is 1 for the case of $c_e < c < c_b$, and in c_b/c case of $c_b < c < c_o$.

$$D_i \approx \frac{R^2}{T_R} \approx \frac{k_B T n_e^2 N_{Mbead}^{3/2}}{\eta_S b N^2} X \tag{96}$$

Here, X is for the case of $c_e < c < c_b$: $(c_b/c)^{1/2}$ and in case of $c_b < c < c_o$: $(c/c_b)^{1/3}$. The decrease of the self-diffusion coefficient in the entangled regime is surprising, and explained by a strong initial entanglement that decreases due to decreasing correlation length, and an increasing bead diameter along with a decreasing chain length, minimizing interaction sites.

$$\eta \approx \frac{\eta_S N^3}{N_e^4 N_{Mbead}^3} X \tag{97}$$

Here, X is $(c/c_b)^{3/2}$ for the case of $c_e < c < c_b$, and 1 in case of $c_b < c < c_o$. Like in case of Eq. (96), the viscosity shows counter-intuitive behavior. The viscosity increases in the entangled regime, but not in the bead controlled regime. This behavior is explained by the low number of interaction sites in the bead controlled regime. In this regime, however two conditions must be fulfilled: 1. n_e of entanglement is similar to n_e for normal polymers; 2. c_e is be below c_b.

This system behaves more like a dilute solution of beads than like a solution of polymers [94]. This behavior opens interesting new possibilities and applications to this type of polymer solution such as being an additive in polymer melts for extruders, reducing the viscosity and at the same time not disturbing properties, e.g. optical properties, since it is a polymer.

By comparing the string and bead controlled regimes, the following conclusions of the necklace structures can be drawn:

1. As long as the system is controlled by strings (string size larger than bead size) the PE behaves like a linear PE and has similar scaling regimes [94].
2. If the bead size reaches similar distances to the string between the beads, then one enters the bead controlled regime with significantly different scaling factors [94].

Adding salt to necklace solutions:
Adding salt to the PE-bead containing solutions changes the PE structure and rheology. An extensive discussion of the structural properties of the PE necklace structure for different salt concentrations as well as the model of counterion condensation on the string and beads can be found in Ref. [94]. This part of the chapter focuses on the rheological properties for these PE in the semidilute high salt concentration region ($c_s > fc$), for the special conditions of low salt ($c_s \ll fc$) and very high salt concentrations ($c_s \gg fc$), see [94]. The relaxation time (longest mode) and viscosity for the high salt semidiluted unentangled regime of the PE necklace in the string controlled region is [94]:

$$\tau \approx \frac{\eta_S b^3}{k_B T} N_{Mbead}^{-3/4} \left(1 + \frac{2c_s}{fc}\right)^{-3/4} (cb^3)^{-1/2} \tag{98}$$

$$\eta \approx \eta_S N N_{Mbead}^{-3/4} \left(1 + \frac{2c_S}{fc}\right)^{-3/4} (cb^3)^{1/2} \tag{99}$$

In the semidiluted entangled regime, the viscosity and relaxation time change to [94]:

$$\tau \approx \frac{\eta_S N^3 b^3}{k_B T n_e^2} N_{Mbead}^{-3/2} \left(1 + \frac{2c_s}{fc}\right)^{-3/2} \tag{100}$$

$$\eta \approx \eta_S \left(\frac{N^3}{n_e^4}\right) N_{Mbead}^{-9/4} \left(1 + \frac{2c_S}{fc}\right)^{-9/4} (cb^3)^{3/2} \tag{101}$$

In the bead controlled unentangled region, the dependence of the viscosity and relaxation time (longest mode) on the concentration and ionic strength (high ionic strength) is [94]:

$$\tau \approx \frac{\eta_S}{k_B T} N^2 N_{Mbead}^{-1} \left(1 + \frac{2c_S}{fc}\right)^{-5/4} c^{-1} \tag{102}$$

$$\eta \approx \eta_S N N_{Mbead}^{-1} \left(1 + \frac{2c_S}{fc}\right)^{-5/4} \tag{103}$$

In the entangled region Eqs. (102) and (103) become [94]:

$$\tau \approx \frac{\eta_S N^3}{k_B T n_e^2} N_{Mbead}^{-2} \left(1 + \frac{2c_S}{fc}\right)^{-5/2} c^{-1} \tag{104}$$

$$\eta \approx \eta_S \left(\frac{N^3}{n_e^4}\right) N_{Mbead}^{-3} \left(1 + \frac{2c_S}{fc}\right)^{-15/4} \tag{105}$$

The free energy of phase separation (bead formation) in such a necklace solution can be calculated via the free energy according to following relation [26, 95]:

$$\frac{F_{neck}(\phi)}{k_B T} \approx \frac{V}{b^3} \left(\frac{\phi}{N} \ln(\phi) + \phi f \ln T_R \beta_c + f\phi \frac{(1-\beta_c)^{2/3}}{3} \left(\frac{K}{f}\right)^{2/3} T_R - \phi T_R^2\right) \tag{106}$$

Here β_c is the fraction of condensed counter ions. Equation (106) was used to calculate the phase diagram of a PE in a poor solvent [95]. The terms on the right hand side are: the entropy of mixing, the entropy of the counterions inside the bead, the free energy of the beads and the monomer-monomer interaction due to short range forces within the beads. The background theory of Eq. (106) is based on Osawa's two zone model of counterion condensation. The increasing concentration of counterions is used to induce a phase separation of the solution, which is dependent on the temperature. The phase separations and, depending on the solution properties, also additional changes of the solution structure, can be measured by changes in the viscosity (see above sections) and/or be followed by SAX or SANS (small angle X-ray and neutron scattering) (see also Sect. 5 for more information about experiments) [95]. Figure 6 shows the solution regimes of PE necklaces in a poor solvent.

3.7 Polyelectrolyte Gels

One interesting feature of PE solutions is the ability of PEs to form cross-linked gel networks [83, 96]. These networks can be formed either by chemical or by ionic thermo-reversible bonds formed by e.g. multivalent ions as cross-linkers [83, 97]. A Flory theory based theoretical study of the PE gelation points using di- and

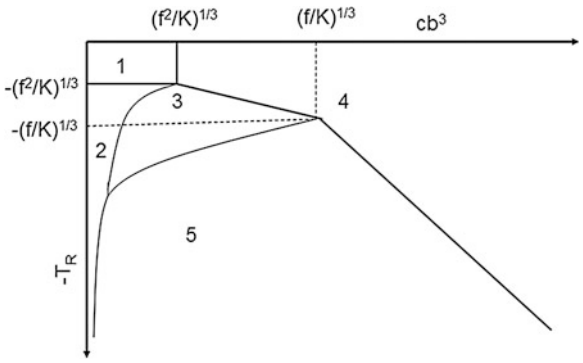

Fig. 6 The different solution regimes of a PE able to form necklaces. Range *1* symbolizes the area of the θ solvent, range *2* the region in which the polymer solvent interaction dominate on small length scales and the PE starts forming the globules of the necklaces. In this region dilute and semidilute regime are possible. In region *3* the PE is in the bead controlled regime while region *4* symbolizes the concentrated solution regime. Region *5* denotes the area of phase separation. Image adapted with permission from Ref. [95]. Copyright 2001, American Chemical Society

tri-valent ions was able to show that the free energy of such a system consists of the translational entropy, the combinational free entropy (entropy of choosing different units) and the free energy of the cross-links [83]. This approach also was additionally able to prove that the weaker the charge of the ionic groups (l_B/a ratio), the more multivalent ions are needed for gelation [83]. If the values of the l_B/a ratio were changed from 5 to 2, the amount of ions needed increased by nearly two orders of magnitude [83]. In a later paper, the same authors were able to show the structural gelation lines of PE gels comprised of different charges and functionalities resulting in different cross-linker energies, and these PE gels were compared with neutral polymer gels [97]. Further, in this study the PE gels in semidilute solutions exhibited a re-entry point of the gelation, which was also described in other models [97].

The same group published another contribution to this topic which describes the complexation of oppositely charged PEs, focusing on the effect of ion pair formation [98]. The free energy was derived from the law of mass action, where the Flory-Huggins parameter was influenced by the polymer fraction [98]. The PE cluster structure, as well as the precipitate properties were described to be salt dependent, which is also in agreement with other theories [16, 98].

4 Computer Simulations and Structure

Experimental methods often require a complicated mathematical treatment to extract the data, e.g. from. X-ray and neutron scattering or reflectometry data, which renders the result not univariant but multivariant [99, 100]. Computer simulations, on the contrary, allow a direct observation of the molecular structure

with the option to photograph it by making screen captures [101, 102]. One of the main drawbacks of these methods is that the size of the systems that can be simulated with quantum mechanics is limited to either a few short PEs or one long chain when using a standard PC due to the high computational demand [103, 104]. This limit will be extended in the near future with the emergence of quantum computers [105, 106], like those manufactured by D-wave Systems [107] which have already successfully proven to be capable of the simulation of protein structures [108]. Due to the currently high price, lack of software and computational results of quantum computers, this review focuses on the computational results of current, standard computers.

Using a coarse grain model for PE structures (averaging the mean field similar to the mean field theory over e.g. the monomer groups of the PE) [103, 104, 109] extends the amount of observable PE chain monomers significantly. The great advantage of using a coarse grain model is that the structural change of the whole polymer, which occurs on much longer timescales compared to changes of single atoms, becomes visible [104, 110]. One of the main problems is that the finite system sizes force scientists to use simplifications (e.g. either salt atoms are neglected or the chain-chain interaction) [103, 104, 111, 112].

The best approach is, therefore, to compare the results of simulations made at different length scales with real measurements to determine the validity of the approach since the causes for changes in e.g. viscosity can be caused by changes in local interaction energy or with the PE structure or both [103]. In this section, the results of computer simulations with relation to the PE structure, complex formation and dilution behavior are summarized. The focus lies on molecular dynamics simulations since Monte Carlo simulations [102, 113] are discussed in detail in chapter 'Thermodynamic and Rheological Properties of Polyelectrolyte Systems'.

4.1 Brief Summary Monte Carlo Simulations and Other Simulation Methods

Since the results of Monte Carlo (MC) simulations on PE structure are discussed in detail in chapter Thermodynamic and Rheological Properties of Polyelectrolyte Systems, only a brief summary of this simulation method and some results related to this chapter are discussed. In addition, a short overview of recent developments in field theoretical approaches is given.

Monte Carlo simulations [102]. are generally less precise in regard to the real reaction time and dynamics of a system compared to MD simulations since MC simulations base on statistics and not real speed of the particles [103]. MC simulations are often lattice based, are easier to program and are also well suited for discontinuous or not differentiable energy functions as well as to define structural equilibration and static properties [103]. With such properties, MC simulations are

well suited for the simulation of the PE conformational structures and also their complex formation [104, 109, 114, 115]. For this reason, simulations of PE-complexes done with MD are very scarce and most PE complexes have been simulated with the MC method or derivations of it, see reviews [16, 104, 109, 116], as well as chapter 'Thermodynamic and Rheological Properties of Polyelectrolyte Systems' for details and corresponding MC based papers. Along with PE complexes, PE gels have also been studied with MC simulation. The focus was on the interaction of the PE gel molecules with strongly charged macro-ions e.g. from surfactants [117]. Other studies focused on the effect of different PE chain lengths as well as polydispersed PE chains in a PE gel, finding that the effect of polydispersity is larger for PE gels than for uncharged gels [118].

Field theoretical approaches have been successful in the area of polymer physics and physical chemistry [74, 77–79]. In particular, for mean field simulations great advances have been made in recent years, as can be seen in the extensive review of Ref. [74]. These advances led also to new developments in the field of PE solutions, e.g. in the simulation of the osmotic pressure of NaPSS solutions [74, 119].

An novel approach is the combination between self-consistent field theoretical approaches and Monte Carlo simulations called theoretically informed coarse grain simulations [120]. It was developed in the field of block copolymers and could easily be extended to PE based copolymers and also thermodynamic calculations [120].

4.2 Molecular Dynamics Simulations

One of the main methods used in computer simulation of explicit atoms, molecular groups and particles is molecular dynamics (MD) [101, 103, 104, 109]. This method allows the simulation of the dynamic movement of particles (atoms or molecular groups), which are usually assumed to be spheres [101, 103, 104]. The special feature of this method is that the movement of these particles is in real time and that each particle has a potential well, which can alter the speed of the particles [101]. This not only allows detailed measurement of self-folding structures, but also the determination of self-folding times, dynamics and temperatures [103]. In contrast to MC simulations which use statistical probabilities and a priori knowledge to determine changes to the system, MD can even be used to simulate the real quantum mechanical probabilities of a atom [103]. Due to the high computational demand and the low observable timescales of these processes, usually molecular groups are merged into a coarse grain model [103, 104].

This part of the book chapter is focused on MD coarse grained simulation results of thermodynamic and rheological properties of PEs. For a detailed introduction into MD simulations and coarse graining see references [103, 104, 109, 121]. MD simulations have been used very successfully in the determination of DNA structures, for excellent reviews of MD coarse graining simulations of these DNA structures and their properties see references [109, 121].

4.2.1 Coupling Constants

The effect of the coupling constant on the PE structure and counterion condensation discussed in Sect. 2 was proven by MD simulations, which showed that an increased coupling constant influences counterion condensation as well as the structure of the PE [122–124].

Monovalent counterions: The effect of counterion condensation at various solvent qualities with different salt concentrations and charge densities have been simulated using PE-MD simulations [125]. By 1995, the structure factor, the coulomb forces, the end to end distances, the polymer and counterion based chain concentration, the osmotic pressure and the persistence length had been simulated by the group of Kremer, and the values were compared with analytical equations and experiments [125]. Later studies of this group extended this approach to poor solvents for strongly charged PEs [126]. The dependence of the degree of polymerization and the monomer width on the crossover point from electrostatic to hydrophobic controlled regime and its effect on the structure factor was determined in this study [126]. The effects of chain ends on PE chains was simulated by Limbach et al. [127] with the result that the chain ends are much more charged than the center of the PE in both strong and weak PEs, as well as in different solvent qualities and ionic strengths. The results of another MD study showed that PEs are not homogeneously stretched supports this finding [128]. Investigations of the effect of counterion concentrations and solvent qualities were able to show the formation of bundles and blobs within PE brushes in MD simulations [129, 130]. Although hard to synthesize for bulk applications, such PE structures in solution could enable new and interesting viscoelastic and/or optical properties.

PSS in water at different degrees of sulphonation, which causes a varying degree of the fraction of charged monomers, showed in atomistic simulations structures depending on the degree of charge (sulphonation) [119]. The transition from elongated to collapsed chains was in agreement with the scaling theory as well as with calculations performed by Kuhn in the 1950s [2, 24, 119]. A coarse grained simulation of strongly charged PEs (a group which includes PSS) was done by Chang and Yethiraj for bad solvents without added salt [122]. In this simulation the solvent parameter was varied from good to bad across a variety of solution phases ranging from dissolved (good to bad solvent) and necklace-bead structures, to phase separation in the case of bad solvents, with various structures depending on the polymer concentration [122]. During these simulations, the structure factor was also determined, and this showed a polymer concentration dependent peak [122].

4.2.2 Necklaces, Poor Solvents and Counterions

The formation of necklace like structures due to poor solvents and counterion condensation was first simulated by the Kremer group and the structure factor was calculated as a function of the wave vector [131]. In a paper about end effects of

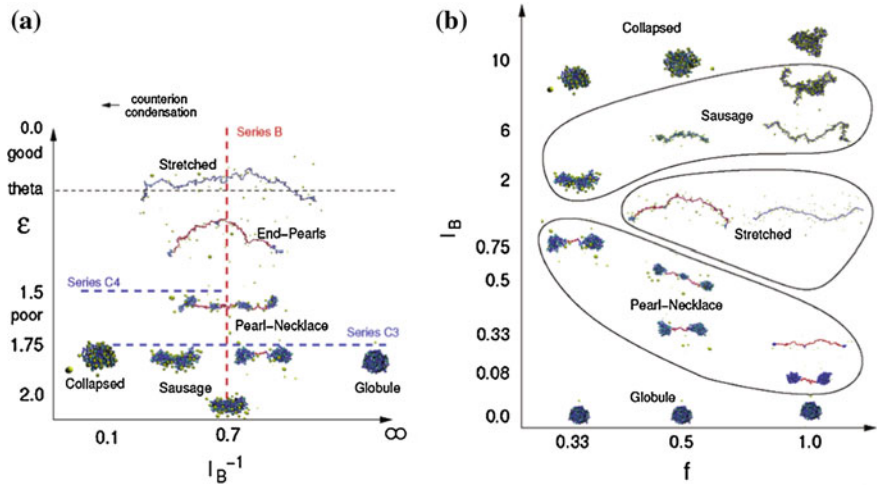

Fig. 7 Chain conformations of a strong PE for varying conditions. **a** Simulated for f = 1/3, showing the influence of the Bjerrum length and solvent quality on the PE structure. **b** Bjerrum length versus charge fraction in a poor solvent. Image reprinted with permission from Ref. [135]. Copyright Americal chemical society 2003

strong PEs, the development of necklaces in poor solvents was reported [127]. The necklaces showed in the middle of the PE a nearly balanced charge, while necklaces at the end of the PE exhibited an overcompensated charge [127]. No instability of the necklaces due to counterion condensation in the dilute regime were reported by other papers, and only minor changes in the form factors have been found [132–134]. These small changes in the form factor are a major hindrance to experimental observations, since the change of the form factor is related to changes in the monomer density of $F_S \propto \varphi_M^{0.35}$ in case of poor solvents, which differs from the structure factor of good solvents of $F_S \propto \varphi_M^{1/2}$ for the dilute and $F_S \propto \varphi_M^{1/3}$ for semidilute phase [133]. In a systematic study of the structural conditions of strong PEs in a poor solvent, the necklace regime was reported to be rather small [135]. In this study only small changes in observable parameters like the form factor could be observed despite large changes in the chain conformation simulated for a large variety of possible influences parameters which included Bjerrum length, Manning parameter, string length, number and size of necklaces, chain length, solvent quality, counterions and their distribution, and polymer density [135]. The results of these systematic simulations are shown in Fig. 7.

The simulation of the dissolution or breakup of a big PE globule (called necklace formation) was done in theory and MD simulation by the Dobrynin and Rubinstein groups [124]. The globule is treated in such a simulation like a Rayleigh drop with a certain degree of outer and inner charge, and the globule breaks down into two evenly sized sub PE globules with the PE chain connecting both globules if the charge surpasses a certain degree [26]. The PE chain bridges

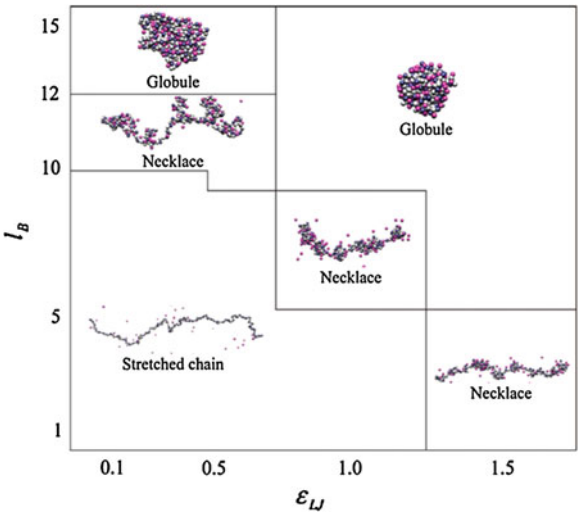

Fig. 8 Counterion mediated necklace formation in a good solvent. The chain conformations were simulated with $N = 304$ and a charge fraction of 1/3. Image reprinted with permission from Ref. [136]. Copyright American Chemical Society 2007

these two globules, which can be split into even smaller globules if the charge is raised further. A convenient summary of the research on PE necklaces in theory and simulation can be found in Ref. [26].

A simple way to form necklaces in good solvents with the introduction of counterions was presented by Jeon and Dobrynin [136]. Such a counterion induced necklace formation was found to be possible by Jeon if the fraction of charged monomers in the simulation was reduced to 0.3 in good, theta and poor solvents [136]. The results of this method are summarized in Fig. 8, which is significantly different from Fig. 7a due to a different necklace forming mechanism and use of different PE.

The theory of the necklace formation for a hydrophobic PE in a poor solvent was done by Liao et al. [124] accompanied by MD simulations which covered different charged fractions, degree of polymerization and different solvent qualities. The MD results support the theory which is discussed in detail in the thermodynamics section of this chapter. The transition regimes of diblock Polyampholytes were investigated with MD and scaling theory by Wang and Rubinstein [137]. They detected three regimes of the electrostatically driven coil to globule transitions, which are known to depend on the electrostatic interaction energy [137].

4.2.3 Monovalent Salt Solutions

The effect of salt solutions on the properties of a flexible PE was investigated by Carillo [138]. It is interesting to note that the results obtained for the persistence length in the dilute regime [138].

$$l_p \propto \frac{1}{\sqrt{[]c_s}} \tag{107}$$

deviated from the ones obtained by analytical considerations, which is shown in Eq. (2), but were in agreement with a definition of the Debye length in Ref. [24]. This contradiction can be explained by different theoretical approaches between the two references. It is worth noting that there are 2 regimes in the semidilute region, one which lasts approximately from 0 ionic strength to $c_s/c_{s0} = 1$ (where c_{s0} is defined as the counterion concentration in a salt free solution) and shows a linear decrease of the Debye length [138]. This regime deviates from Eqs. (2) and (107) because it is still a counterion controlled regime and the amount of added salt is still not significant. The second regime shows a decrease of the persistence length according to Eq. (107) [138]. The chain size in the dilute regime correlates with the ionic strength by $R \propto c_s^{-1/5}$ [138] which is in good agreement with the correlation stated in Ref. [24].

$$R \approx bN^{3/5}(c_p b^3)^{-1/5}(Nb/L)^{-2/5}(1 + 2c_s(N(1-f))/c_p)^{-1/5} \tag{108}$$

The scaling of the decrease of the chain size with increasing polymer concentration correlates with $R \propto c_S^{-1/4}$, which is in agreement with current scaling laws, which predicted a similar exponent [24, 138]:

$$R \approx L\left(\frac{c_P}{c^*}\right)^{-1/4} \tag{109}$$

A weaker correlation of $R \propto c_S^{-1/8}$ was found for high salt concentrations, which might be caused the fact that the chains were already quite contracted due to the high ionic strength [138]. The correlation length to salt concentration determined was $\zeta \propto c_S^{-1/2}$, which is in line with Eq. (11) and Ref. [24].

4.2.4 Divalent Counterions

The effects of divalent counterions investigated by Brownian dynamics studies showed that the same concentration of divalent counterions caused a stronger chain contraction, a stronger self-diffusion and a stronger scattering peak compared to monovalent counterions [38].

4.2.5 Multivalent Counterions

The bending rigidity and counterion condensation was investigated with a langevin simulation method with the possibility to insert an arbitrary counterion valency [123]. A detailed investigation of this study showed that, if the Bjerrum length

comes in the range of the bond length, the counterions enrich in an imaginary tube around the polymer and not only coils and rods, but also thyroids can emerge [123].

4.2.6 Weak Polyelectrolytes

One of the few MD studies of weak PEs eas done by Konieczny et al. [139]. In this study, the effect of the PE solution without added salt and a charge degree below 20 %, which is below the Manning counterion condensation limit, was assumed [139]. The PE structure was compared with analytical calculations, and good quantitative agreement was found [139]. In the case of a charge >20 %, the PE structure changed from coil to rod and the analytical considerations did not apply anymore [139].

4.2.7 Enthalpy and Entropy of Polyelectrolyte Complex Formation

The thermodynamic properties of two PE molecules of same charge density in the dilute regime of a good solvent with added salt were calculated theoretically and simulated by Langevin [19]. In this study the enthalpy was determined by changes of the coulomb energy before and after the complex formation, while the entropy was determined by the counterion release [19]. The system showed, in case of strong PEs, an entropy controlled complex formation due to a positive enthalpy, while it showed for weak PEs or strong dielectric solvent an enthalpy controlled complex formation due to a negative enthalpy [19]. The authors pointed out that the addition of salt significantly affects the enthalpy of strong PEs and weakly affects the entropy of the released counterions [19]. The functions used by the authors are shown in the above thermodynamic section.

Another study in the field of PE complex formation covered PE-polyampholyte complexes. The resulting structures of this type of complexes were dependent on the structure of the polyampholyte (dibloc, or polyblock) as well as the ionic strength and polymer concentration [140]. The simulation was additionally treated theoretically by a calculation of the free energy based on the Flory theory [140]. In a subsequent study, the same authors discussed the effect of a poor solvent and different ionic strengths on different types of polyampholytes (di-or polyblock) [141]. It was shown that the PE can either form a globule with the polyampholyte or the PE can wrap the polyampholyte, depending on the polyampholyte composition and the ionic strength, resulting in different structure factors [141].

4.2.8 Adsorption of Polyelectrolyte Chains and Formation of Thin Films

The adsorption mechanisms of PEs have been more extensively studied than pure PE complex formation. This, on first glance, contradictory way of studying PE complex formation is result of the large success of layer-by-layer thin films and their large potential in science and applications [6]. Since this topic is only partly related to this book chapter, it is only briefly summarized here.

The adsorption of PE chains on negatively charged surfaces using the example of cellulose surfaces was simulated and compared with AFM images in the PhD thesis of Biermann [13]. The group of Dobrynin investigated the wrapping of dispersed nanoparticles by PEs [142]. The buildup of PEM thin films was investigated by the same group by taking electrostatic, short range interaction, polymerization degree, charged fraction and diffusion into account [143, 144]. In this way it was possible to show that there is a transition from linear to exponential growth of these thin films [143, 144]. The PE adsorption process was investigated in more detail in subsequent publications by the same group by taking the solvent quality, surface charge and surface overcharging into account [145]. In later publications, the adsorption of PE films on nanoporous substrates as well as different salt solutions were also taken into account [138, 146]. The swelling effect of crosslinked PE thin films was investigated by other groups by calculating the osmotic pressure within the PE crosslink complex, which is partly influenced by trapped counterions [147–149].

4.3 Viscosity of Polyelectrolyte Solutions

It has not yet been possible to directly determine the viscosity values of PE solutions by MD simulations. This is because of the difference in time and length scales between the molecular properties and the macroscopically observed regime [74]. It is, however, possible to determine and simulate microscopic effects that have a large influence on the viscosity or to simulate an environment that is constrained so that a viscosity can be determined or extended to the solution regime, although only within a very narrow concentration regime. Such work was done by Carrillo et al. [112] by simulating the shear viscosity of charged bottle brushes for different pressures and grafting densities. The PE brushes exhibited a lower shear viscosity as well as different behavior compared to neutral polymers, which is in agreement with experimental findings and current theory [112] (see also Fig. 9).

The degree of shear thinning was found to depend on the degree of backbone deformation, which is much higher in case of neutral polymers [112]. Another way to deal with this problem, and to avoid the introduction of additional surfaces, is to determine molecular effects that have a strong influence on the PE viscosity like the Rouse dynamic relaxation times [150]. This specific parameter was studied by

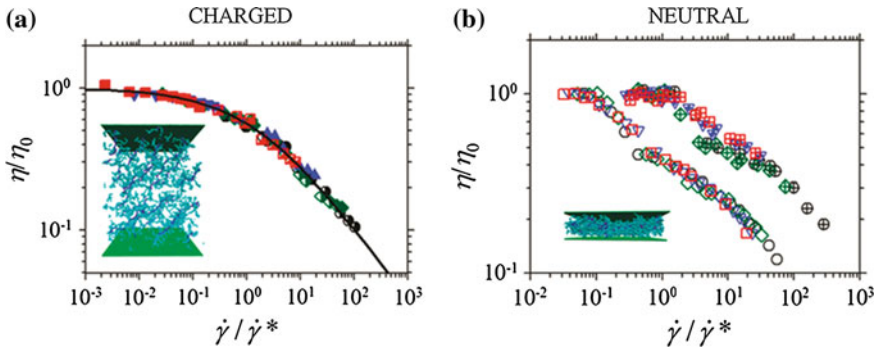

Fig. 9 Molecular dynamics simulation of charged bottle brushes versus neutral polymers, shear viscosity versus shear rate of **a** PE brush and **b** neutral brush, image reprinted with permission from Ref. [112]. Copyright American Chemical Society 2011

the Dobrynin group with a MD bead spring model, which follows the Rouse model by taking counterions as well as different charge degrees into account [150]. In the dilute solution regime, the relaxation time increased exponentially with the chain length $\tau_{RR} \approx N^3$, which was found to be higher than the value obtained from the scaling regime (Eqs. 65, 66), but it was in line with values from entangled regimes (Eq. 82) [150]. The result for the semidilute region, $\tau_{RR} \approx N^2$, was in agreement with Eq. 66 [150]. The relaxation time decreased with increasing polymer concentration due to chain contraction, which depended in the dilute region non monotinically, and in the semidilute region with the exponent $\tau_{RR} \approx c_P^{-1/2}$, on the PE concentration [150]. Such a concentration dependence is in agreement with the scaling theory as can be seen in Eq. (77) [150]. At high polymer concentrations the authors reported an increasing relaxation time, which was explained with an increase of the monomer friction coefficient [150]. It is interesting to note that the authors also determined the self-diffusion coefficient, which also affects the viscosity and depended on the concentration but not on the chain length [150]. The self-diffusion coefficient was also determined by other groups with Brownian MD for short chain PEs in dilute salt free solution, taking long-range hydrodynamic and coulomb interactions into account [151]. The whole chain diffusion was found to be related differently to the coulomb interaction than the short time Kirkwood diffusion which is related inversely to the chain size [151]. This relation to the coulomb interaction proved the importance of taking the hydrodynamic interaction into account [151].

The effect of shear thinning and molecular orientation of uncharged short chain polymers was simulated by Pierleoni et al. [111] in 1995. This simulation showed that the shear thinning is able to destroy blobs (although, due to the short chain length, only 1 blob was present) [111]. According to this report, the amount of blobs per chain, N_B, the blob size and the relaxation time in a polymer solution under shear are inversely dependent on the shear rate [111]:

$$N_B = N\beta_R^{-1/3\nu'} \tag{110}$$

$$\tau_n \sim n^{3\nu'} \sim \dot{\gamma}^{-1} \tag{111}$$

Here $\nu' < \nu$ with ν being the Flory exponent. β_R being a large reduced shear rate ($\beta_R \gg 1$), and $\dot{\gamma}$ being the shear rate. Also the birefringences and structure factor were estimated. These results are also able to explain the shear thinning effects in PE solutions [27, 152], which can (up to now) not be explained by the scaling theory or by Rouse dynamics [27, 152].

An interesting Monte Carlo simulation with embedded dissipative particle dynamics showed that the PE radius of gyration can shrink and swell depending on the concentration of salt added and the solvent quality [114].

PE gels were also investigated by MD dynamics studies. One extensive study of this interesting subject was performed by Pablo [153]. In this study, a crosslinked PE network was assumed and its interaction with mono-, di- and tri-valent counterions were investigated [153]. The osmotic pressure, structure factor, the elastic entropy (which was found to behave nearly classically) and Bjerrum length were calculated [153]. The discontinuous phase transition of PE gels was explained by the authors with the interplay of the elastic energy of the PE chains and the entropy of the counterions [153]. The structure of the PE gel was found to consist of nearly fully extended chains in the swollen state, and chains in a Gauss like state in the collapsed state [153]. In this collapsed state, the internal osmotic pressure of the PE gel was found to be higher than in the extended state [153].

5 Experimental Characterization

The structure of the PE, as mentioned in the computer simulation or theoretical section, has seldom been directly observed. Such a direct observation is, in principle, possible by high resolution TEM, or in case of dried solutions, by AFM as some recent AFM studies demonstrated for non charged polymer brushes in different solutions with different Flory-Huggins solubility parameters [154]. To ensure a measurement in non disturbed conditions, in most cases some indirect measurements, like small angle neutron scattering, X-ray scattering, light scattering, simulations, viscosimetry, or, if one employs proper dyes, also spectroscopic methods, can be employed for observing the features discussed above. This section discusses the different methods for each type of investigation and their relation to the parameters determined. The PE experimental methods of this section are divided into: viscosimetry, scattering techniques and spectroscopic approaches. Electrical measurements are omitted from this section.

5.1 Viscosimetry and Rheology

The effects of a different viscosity behavior of PE solutions compared to apolar polymer solutions was first reported in a book edited by Staudinger, as well as in a publication of Heidelberger in the 1930s [155, 156]. In the following decade, the scaling of the viscosity as a function of the concentration was determined for PE solutions by Fuoss, where the scaling for apolar polymer solutions was determined by Staudinger [17, 157, 158]. The methods and calculations for high precision viscosity measurements as well as for the relaxation times are described in detail in the publications of Adam and Delsanti [87, 88]. Another high precision viscosimeter designed for measuring highly diluted PE solutions was developed by Cohen [159].

At this point it is worth mentioning that the absolute viscosity of PE solutions up to the entanglement concentration is much higher than the one of uncharged polymer solutions [27]. Only the increase of the viscosity upon increasing concentration is lower compared to apolar polymers. This effect is not mentioned in most publications since most publications just compare PE with each other or even use different units [27]. The first contribution known to the authors actually comparing PEs with apolar polymers using the same units was Colby in 2009 [27]. Another problem when dealing with data interpretation is the mixing of the entanglement and the overlap concentration which was, in some old papers, referred to as being the same [27].

Polyvinylpyridonium (PVP) and polyvinylbutyl-pyridonium in water, ethanol and mixtures of these two solvents at different pH and degrees of ionization were used by Fuoss to validate the consistency of his approach [158]. PmAA (polymethacrylic acid) at different ionization degrees was investigated by Kuhn, and it was found that the viscosity increased with increasing ionization [2]. The effect of adding salt to strong PEs causes a similar effect to decreasing the degree of ionization of weak PEs [159, 160]. The viscosity of cellulose sulphate (strong PE) can be switched from exponentially decreasing, to linear, to exponentially increasing viscosity upon increasing PE concentration, depending on the ionic strength of the solution [160]. This effect can be explained with different degrees of interaction and charge shielding effects of the PE with its surrounding ions and other PEs [160].

PE solutions without addition of salt can also form regular structures that can be detected by viscosity measurements [159]. By plotting the reduced viscosity versus the logarithmic concentration, Cohen was able to detect the strong dependence of the PE viscosity on the concentration, with a maximum of the specific viscosity at $\sim$10–5 mol/L [159]. The height and position of the peak maximum depended on the molecular weight, where an increasing molecular weight shifted the maximum of the peak to higher concentrations, and the peak became more pronounced (see scattering and theory sections for more information about PE structures) [159].

The counterion association with the PE also influences the degree of charge, meaning that a stronger association causes a lower ionic PE–PE interaction and therefore lower viscosity [161]. The minimum in the reduced viscosity for a salt free solution of 0.45 N PSS solutions can be explained by the dissociation and mobility of the counterions [161]. Another study of PSS was done by Zebrowski and Fuller, who investigated the relaxation times of this PE. In their paper, a decreasing relaxation time for an increasing PE or salt concentration was reported [162]. In addition, an increasing deviation of the Zimm like behavior at a decreasing PE concentration and PE charge (which can be decreased by increasing the ionic strength) was found [162]. Such a deviation of the Zimm like behavior can be explained by the effect of ionic charges on the PE, which is not included in the original Zimm model [163]. This work was extended by Boris and Colby who increased the concentration range of the PE solutions investigated, and detected that the onset of shear thinning and viscosity is inversely proportional with the relaxation time [164, 165]. In addition, they also found that the fact that the Fuoss law only applies at higher shear rates [164]. A maximum in the relaxation time was found to be at 2×10^{-4} mol/L, and the relaxation time increased again after reaching the entanglement concentration [164]. Such a behavior was not forecast by scaling theory, but was also detected for different PEs and has, to the authors knowledge, so far only been explained in a narrow concentration range [27, 164]. The same effect is true for the modulus [27, 164]. PSS solutions were investigated in salt free solutions by Chen and Archer and unexpected relaxation times, which were caused by PSS aggregates and coupled polyion diffusions, were detected [166]. The inverse dependence of the relaxation time on PE molecular weight for low concentrations could not be explained by their data or by aggregation [166].

Charge density effects on PE solution rheology and solvent properties were investigated by Dou and Colby by measuring the rheological properties of PVP solutions in a good solvent at different PE concentrations [167]. They found the dependence of the chain overlap concentration on the charge density of the PE, which was also in agreement with the theoretical model of Dobrynin [26, 167]. Other measured parameters like the modulus or the relaxation time dependence on the concentration and charge density were in line with the scaling and the observed trends were reproduced theoretically [167].

The onset point of the shear thinning effect of PE solution depends on the inverse of the relaxation time of the PE chain [152]. It is interesting to note that the shear thinning effects in the study of Krause were found only for high molecular weight samples, and therefore no exact relaxation time could be determined [152]. Generally, the trend of shear thinning can be explained by an extension of the PE chain by shear force, and the viscosity is proportional to the size of the chain cross section that is exposed to the flow, as defined by the Pincus blob size, $\xi \sim \dot{\gamma}^{-1/2}$, and therefore $\eta \sim \dot{\gamma}^{-1/2}$ [165]. This behavior was explained with a modified Rouse model and Cox-Merz empiricism [165]. In steady state shear and oscillatory shear the relaxation time modes that are longer than $\dot{\gamma}^{-1}$ do not contribute to the steady

state or dynamic viscosity, and therefore lead to a decrease in the detected viscosity [165].

Amphiphilic and hydrophobically modified PEs were investigated by Di-Cola with various techniques [168]. The increase in viscosity upon increasing concentration was determined to be $\eta \sim c^a$, where a was 0.5 in case of semidilute unentangled and 1.5 in the entangled regime [168]. When the concentration reached the values at which the intramolecular globules overlapped, the specific viscosity increased by the factor $a = 4$ [168].

Studies of non organic PEs are quite scarce. Some of these studies of inorganic PEs were done by Strauss in the 1950s on polyphosphates with a molecular weight ranging from 7,000 to 19,000 [169, 170]. The short branch points of freshly prepared polyphosphates are not stable and needed some time to decay, and therefore the experiments were performed after a conditioning time [169]. The PE viscosity was found to increase nearly linearly with increasing molecular weight [169]. In a subsequent publication it was shown that inorganic PEs also follow the Fuoss equation [170].

At the end of this section on viscosity, a general problem for the measurement of PE solutions without added ionic strength is mentioned. As pointed out by Colby [27], the overlap concentration of PEs is quite small and there are salt residues at the air- water-interface due to the evaporation of water [159, 164]. Therefore deriving values or the interpretation of data can produce errors if the experiment and equipment is not designed carefully. The viscosity properties of PE complexes are discussed in the PE complexation and gel section of this chapter.

5.2 Scattering Approaches (Light, X-ray, Neutron)

It is interesting to note that reports about birefringences caused by PE solutions under shear flow were published in 1948 [2]. In these reports the influence of the molecular confinement of the PE in solution, and the degree of ionization of the PE on birefringence properties had already been taken into account [2]. The absolute value of the birefringences depends not only on the geometry but also on the polarizability and anisotropy of the polymer [2]. This theory was proved in 1988 by experiments with PSS in 95 % glycerol at different NaCl concentrations by Fuller and Zebrowski [162]. An increasing ionic strength led to decreasing birefringences in the equilibrium state of the PE solution, and is known to decrease the PE linear structure due to a shielding of the charges [162]. The birefringences were found to increase upon increasing shear modulus [162]. Such behaviour was explained by the authors by a decoiling of the PE chains due to shear force, which is in agreement with MD simulations [111, 162]. An overshoot in the birefringences, observed for low ionic strength, was explained as an effect that emerges when the relaxation time is larger than the reciprocal shear time [162]. Therefore the chains are unable to change their orientation fast enough to the proper position and overshoot in their alignment [162]. This effect was observed to reach its

maximum at 0.002 M NaCl [162]. Light scattering experiments were utilized for a determination of whether PE agglomerates were present or not [162]. Such agglomerates were found in salt free solutions of PSS at concentrations <10 mg/mL [162].

It is interesting to note that not only differences in refractive indexes, but also relaxation times, can be determined by the birefringence method [166]. The laser birefringence detection method is presented in Ref. [166]. Details of the necessary calculations and a comparison of the results obtained compared with rheological methods are also shown are shown in Ref. [166].

Numerous SANS (small angle neutron scattering) experiments with various parameters were used by De Gennes to establish his scaling theory [171, 172]. In these experiments, a peak was found which becomes broader and moves to higher q values (smaller structural sizes) with increasing PE concentration and, in case of increasing salt concentration, a loss of structure [171, 172]. In some cases a completely deuterated PE was used to gain a better contrast of the PE in aqueous solvents [172]. For example, the results of De Gennes and his group's X-ray and neutron scattering were also used by Pfeuty to verify theoretical approaches [53, 89]. The finding that that the scattering peak decreases upon increasing ionic strength was also confirmed by the SANS and SAXS experiments of Essafi et al. [173] and Bordi et al. [174]. The decrease of structure was attributed to an increase of polymer density fluctuations [173]. In scattering experiments with poly(acrylamide-co-sodium-2 acrylamido-2-methylproanole sulphate) at different ionic strengths, the scattering peak at q $\sim$0.1 was determined to be correlated with the charged fraction [173]. The interdiffusion between PEs in PE complex based layers (PEM) was investigated by Loesche et al., using neutron reflectometry and deuterated layers of PSS [175]. A PE interdiffusion of up to 3 bilayers ($\sim$1.5 to several nanometers depending on the preparation conditions and type of PE) was reported [175].

Hydrophobic modified PE showed, in the scattering experiments of DiCola, a better resolution for the q range and a wider angular range in X-ray than in neutron scattering [168]. The correlation length scaled with c^{-a} where a was 0.5 in the unentangled, and 1.5 in the entangled regime [168]. In the case when hydrophobic micelles overlap, a was determined to be <0.3 [168].

Light scattering experiments were done by Strauss and Smith on inorganic PEs [169]. A linear increase of scattering intensity upon increasing PE concentration was determined, and the total intensity decreased with increasing ionic strength [169]. The most surprising findings were that the scattering factor, B, and the viscosity were in a linear relationship, and that the charge degree of the polyphosphate was so low that the Donnan term was irrelevant [169]. Light scattering experiments to investigate the effect of the PE structure on the diffusion coefficient were done by Drifford [176]. In this publication, an increasing concentration of PSS was reported to cause a decreasing PE structure, which is in agreement with SANS measurements [168, 176]. For the maximum PE concentration investigated, Drifford determined a minimum diffusion coefficient, though it has to be pointed out that the maximum concentration was overall quite low [176].

Ellypsometric measurements of PE mulitlayers (PEM) comprising PSS and PDDA formed in the presence of salt, showed that PEM exposed to mechanical stress can undergo humidity dependent swelling instead of compression [48]. Such effects were strongly dependent on the preparation of the PE complex, since the composition of the PE complex (polycation to polyanion and counterion ratios) depends on the preparation conditions [69]. In the case of no added salt, the PE film did not show a swelling, but in the case of added salt, it increased in thickness since the polyanion to polycation ratio is not 1:1 and the glass transition point could be surpassed due to the introduction of mechanical energy [39, 69, 71].

5.3 Spectroscopic Approaches

Another way to determine the PE structure is via the excimer (excited dimer) formation of pyrene labeled PE. This way it is possible to determine the coiling of a PE, pH dependent structural change, PE complex formation, interaction with surfactants (these also disrupt excimers), changes in the chemical structure of pyrene labeled PE, and labeling degree of the PE [35]. The details of these methods are listed in review [35]. Changing the pH of pyrene labeled polyethylenimine (PEI) in an aqueous solution from pH 10 to 1.5 causes a general increase in fluorescence, and this is 50 times lower in the excimer than in the monomer [34]. This pyrene fluorescence based PE system not only utilizes the pyrene excimer formation as a label for the PE coiling but also the total fluorescence intensity, since the PEI aminogroups quench the pyrence fluorescence and therefore serve as PE density indicators [34]. The pyrene coiling index, which describes the degree of intramolecular coiling of a polymer chain was investigated by labeling PAH with pyrene [177]. It is defined as the fluorescence intensity ratio between the excimer to monomer fluorescence intensities [177]. The coiling index was tested by varying the charge density of the weak PE, PAH, by varying the solution pH [177]. The main motivation of using pyrene as a label was to enhance the hydrophobic properties as well as serving as a label for the PE structure [177]. The PE adsorption was found to be in a stretched condition, and in the form of a dense layer on the substrate, in which the PE recoils during the PEM assembly, leading to a coagulated PE complex [177]. More uniform, flatter and smooth films were achieved by increasing the ionic strength of the solution [177]. The typical “odd-even” effect which defines contraction and extension of a PE complex film every second bilayer, due to an intrinsic charge compensation and overcharging processes was also observed in this study [69, 177].

Upon mechanical elongation of PEM comprised of pyrene labeled PSS and non labeled PDDA, the PEs were found to decoil due to the shear forces, which is in line with other investigations and simulations [39, 111, 165]. During this decoiling process an increase in local polarity was detected by the same group, which was, in the case of PEM, assembled without the presence of salt, even higher than the polarity of water [39]. This finding was explained by the water within the PEM

having an ice like structure [39]. Such an explanation is in agreement with other studies that detected an effect of PE on water rotational motions [174]. Upon drying, the PEM shrinks, and the drying stress itself was found to lead to decoiling of the PE chains [39]. Absorption spectra of the same type of film proved the local polarity of PEM produced in presence of salt to be inhomogeneously distributed, while that of PE complexes produced without added salt is homogeneous [41]. The inhomogenously distributed local polarity of the PEM is probably induced by a larger degree of interdiffusion, stronger hydrophobic surface effects due to shielding of the charges, or due to the preparation mechanism since the PEM film with added salt is softer [41].

Another spectroscopic method which was applied to PE solutions was dielectric spectroscopy. The theory, as well as a short review of the work of Ito [178], was published by Bordi [174]. Frequency ranges from MHz to GHz were used for the investigations of PE solutions [174]. In this frequency range, waters' rotational motion easily keeps up with the dielectric field and the PE is frozen in space, therefore the conterions can be investigated [174]. In addition to the main results for this intermediate range, a change in the maximum absorption frequency of the water ($\sim$17 MHz) was found when PEs were added to the water, hinting that the PE affects the rotational motion of the water molecules [174]. Below 1 MHz, the PE is relaxed, making it possible to investigate the mode structure of the PE chain [174]. A simple determination of the PE charge fraction and solvent quality, and with additional knowledge (e.g. diffusion coefficient), also the correlation length and polarizability can be determined by this method [174]. The relaxation time of the counterions decreased by factor 200 when the PE concentration was increased by factor 10 in a study of Bordi [174]. The fraction of charged monomers was found to be dependent on the PE type and concentration [174]. Some PEs were found to increase their fraction of charges upon increasing PE concentration like PSS and PAMS, while others like PAMS-80r-PA20 do not [174]. The solvent quality was also found to be affected by the degree of the charged fraction [174].

Dielectric spectra of divinylpyridine (PMVP) from 1 kHz to 2 GHz in water, ethyleneglycole and mixtures of water and ethyleneglycole were investigated by the same authors [179]. The influence of the dielectric increment, relaxation time of the ions as well as the solvent quality were compared with scaling theory, verifying the predicted exponent [179]. Also, the crossover concentration of the PE was in agreement with the predicted values when taking the degree of charged fraction into account [179]. The same authors used this type of measurement to determine the charged fraction of the same PE in ethyleneglycole [179].

6 Polyelectrolyte Complexes and Gels

This section is not intended to be a complete review of this type of materials as there are already other excellent reviews in this field. This section is intended to inform the interested reader of why and how PE complexes are related to

influences in the viscosity. Further, this section shows the reader interesting applications of PE complexes and gels, and where to find further information about this topic.

6.1 Polyelectrolyte Complexes

Aqueous solutions of PE complexes are applied in many fields of science and technology, ranging from drug delivery to coatings for foods [4, 180]. Since a large number of PE complex properties have already been mentioned in previous chapters, this section summarizes work which is closer to applications. In later parts, this section introduces PE complexes based on their applications to show examples of applications and uses of the previously mentioned properties of PEs.

A detailed description of the preparation methods of PEI and PAA complexes was published by Mueller et al. [181] they investigated the influence of the pH, the molecular weight and the mixing with a model drug [181]. When one of the complexes is formed, a small primary complex is formed first, then the small primary complex rapidly agglomerates into a so called secondary PE complex which consists of hundreds of primary complexes [181]. If such small primary complexes are weakly charged, then the resulting secondary particles are usually more strongly charged than the primary complexes [181]. The size of the complex also scales with the molecular weight of the PE, and so the utilization of higher molecular weight PEs results in larger complexes [181].

Three dimensional aggregates of PSS-PDDA complexes were found to exhibit a porous structure with pore sizes on the order of tens of micrometers [182]. Such pores can be closed upon extraction of water in e.g. PEG, where trapped ions stay within the PE complex and cause a re-swelling and restoration of the pores upon reintroduction of water [182]. The PE complex becomes much harder upon drying, with a kinetic component in the first minutes upon applying mechanical force, which then decays [182]. Such a kinetic component, which is caused by chains sliding and decoiling, is in agreement with other studies of PE decoiling in PEM upon elongation and kinetics in PEM-carbon nanotube networks [39, 182, 183].

PE complexes made out of chitosan and xanthan were found to exhibit pH dependent complex formation. At pH 1.5, only 21 % of the PE form complexes, while this increases to 98 % at pH 6.3 [184]. The fibril structures of the complex exhibited sizes from 50 to 100 nm, with pore sizes ranging from 100 nm to 1 μm, making the formed gel like structure suitable for drug and enzyme encapsulation [184]. The enzymes showed a very different behavior—some exhibited an increase in activity, while others a decreased activity in the encapsulated state [184]. This behavior is probably caused by a reaction to steric hindrance as well as a change in the water structure, and dielectric and ionic fields in such a complex network compared to solution.

An interesting review of chitosan PE complexes was written by Hamman, therefore this chapter only briefly summarizes the properties of chitosan and

recommends the review of Hamman for details [5]. Chitosan is a natural, positively charged PE, which is non toxic, cheap and biodegradable; it even can be dissolved in the stomach [5]. Chitosan PE complexes are usually made out of common industrial PE, as well as a large variety of natural PEs, like DNA, xanthan gum, cellulose and its derivates, dextran sulphate, and polyphosphate [5]. A variety of enzymes (e.g. lysocyme), as well as small molecules like insulin were investigated for drug delivery [5, 185]. Other enzymes were investigated for determining structural changes or enzymatic activities in the complex states [5]. Chitin complexes with xanthan gum were even used to form gels, which exhibited the rheological storage modulus of solids [5].

The stability of PE complexes in solution was investigated surprisingly late [186], given that coacervation was first reported in the 1920s [55] and then again in the 1950s [62], and PE structures have been investigated in detail since the 1930s [155, 156]. In recent publications, PEI-Plasmid DNA complexes were freeze-dried at different freezing speeds, freezing with temperature hold steps and at different sucrose concentrations [186]. The temperature hold step was shown to negatively affect the PE complex stability (determined by an increased swelling size after thawing) by mechanically damaging the PE complex due to the formation of ice crystals [186]. Repeating the freezing progress was found to damage the PE complex further [186]. It was further reported by the same authors that agglomeration and complex formation depends on the system's viscosity, and the reaction rate has a critical temperature at −18 °C (freezing of ice was decreased due to the introduction of sucrose as well as controlled ice nucleation) [186]. The reaction rate was found to correlate inversely with the system's viscosity, whereby the reaction rate first increases with time, but decreases rapidly, as soon as the viscosity increases [186].

An interesting study about the influence of various PE effects in particles of poly-L-lysine and chitosane on competing polyanions like DNA and xanthan showed no relative preference of polyanions due to the strong influence of electrostatic forces [187]. The release of ethidium bromide as a marker for ion exchange processes was observed to be quite fast ∼1 min [187]. Further experiments showed that PE can be destabilized depending on the type of employed PE, showing that the complex stability can be PE specific [187]. A study about the speed of PE complex formation of chitosan/DNA complexes showed 3 effective times [188]. First, the diffusion limited part, which is around 5 ms; then the exponential growth part, which is from 5 to 1,000 ms; and then, after 1 s, the gaussian chain parts reorganize [188]. This study was investigated by employing spectroscopic techniques of fluorescence energy transfer to quantum dots [188].

The coating of food like apples and peaches was investigated by using pectin based complexes, where the PE coating was optimized for permeability of gases like oxygen, carbon dioxide, water vapor (which was minimized), antimicrobial properties, controlled release and their digestive properties [180]. The favored PEM complex was a pectin, alginate calcium matrix [180].

Other possibilities to use PE complexes are to utilize them as viscosity enhancement agents [11]. Carboxymethyl-cellulosis and polyaryl-amide-co-dimethylammonium

chloride in various mass ratios, at different temperatures and shear rates were investigated by Zhang et al. [11] to determine the viscosity enhancement rates of the PE complexes. The viscosity enhancement factors obtained (a factor calculated from differences between theoretical and real viscosity) of up to 20 enable a variety of applications for this type of PE complex like agents in the mineral or oil industry, food processing, pharmaceuticals as well as in the cosmetics or textile industry [11].

Other applications of PE complexes are gene delivery systems, by using PE complexes of positively charged PE and negatively charged DNA [4]. One such system comprises of DNA and PEI (polyethyleneimine) complexes, which were additionally coated with alginate to prevent agglomeration of red blood cells to the complex [4]. Such a system with a complex size of 280–360 nm was shown to exhibit low toxicity (up to 50 volume% of such complexes showed no damage to cells in vivo and in vitro). The viscosity of the complex solution could be decreased by decreasing the molecular weight of the PE complexes, as the gene delivery of low viscosity complexes was found to be the highest [4]. The swelling and rheological properties of chitosan and xanthan gum were investigated by Magnin et al. [189]. The coacervation time, molecular weight, pH and acetylation degree were investigated [189]. An increase in coacarvation time resulted in a higher density of the network and therefore a decreased swelling of the PE complex, as an increasing pH led to increased swelling (except for pH 1, which might be strong enough to cleave the chains) [189]. It is interesting to note that the storage modulus of PE complexes that gelate increased up to 10^4 s, and gels immediately harden out [189]. A mechanical mixing of the complexes or gels induced a structural change of the complex [189]. The swelling degree of the complex gel obtained was found to be between 600 and 20,000 % while exhibiting a porous structure, which is favorable for drug delivery [189].

6.2 Polyelectrolyte Gels

PE gels are used in many applications starting from basic food products (gelatin, agar, pudding) and water treatment to oil production agents for fracking [14]. Like Sect. 6.1, this section is not intended to give a full review since other recent reviews summarize this field already [96]. This section is merely intended to introduce effects between PE complexes, as well as PE with multivalent ions and show applications.

The PE behavior in the presence of multivalent counterions was studied by Ermoshkin [83, 190]. Multivalent ions can act as bridging agents between PEs, where strong short-range attractions can facilitate gelation [83]. Such a gelation can be hindered by long range electrostatic correlations from e.g. non crosslinked monomers or ions [83]. Strong diluted PE solutions preferably segregate, while semidilute PE solutions are able to gelate when the distance between charged monomers is higher than the ion size [83].

For non geochemists, a very surprising application is the use of PE complex gels for subterrain gel formations to facilitate hydrocarbon extraction [14]. For such applications, PE complex nanoparticles made out of chaitosan and dextran sulphate with zinc as the crosslinking agent were used [14]. Such complexes showed depending on their concentration and size, an increase in viscosity due to gel formation after 9–12 days [14]. The gel formation could be facilitated up to 60 °C, which allows a large variety of drilling holes, since the temperature in the boreholes spans from 10 to 180 degrees [14]. The same material with additional alginate and PEG (polyethyleneglycole) was used for oral delivery of Insulin in form of acid proof nanogel capsules, where a replacement of the alginate by albumin showed a preferable decrease of the viscosity [185].

A interesting review paper about the fundamental aspects of PE gels, summarizing most of the important achievements in this section was published by Kwon et al. [96]. A short summary is presented here, and the review paper is cited for the readers' convenience. PE gels can achieve a water uptake of up to 2000× their own weight [96]. Due to the high rate of water uptake, they are not only useful as water absorbers, but also as soft and wet cell scaffolds [96]. They also exhibit unique electrical properties, like shape and movement changes upon application of electrical current. This is similar to muscle cells, and they are therefore also called artificial muscles [96]. PE gels can additionally bind their counterions in a so-called potential valley which traps them as the binding energy is larger than the thermal energy [96]. In this context it is not surprising that the water molecules in such potential valleys are hindered in their movement as well [96]. The total number of counterions also increases with the crosslink density, affecting the PE gel's conductivity [96]. The PE units in the gel show a decreasing relaxation time upon increasing concentration, which is comparable to those in solution [96]. Surfactants can not only stick with their apolar group, but also with their ionic group to PE, and even induce a collapse of the gel. Such a collapse can be hindered by adding salt and shielding the electrostatically driven process [96].

7 Conclusion and Outlook

PEs, which were in the past also considered colloids [191], have been investigated for a long time [191], partially under a different name, and sometimes patented rather than published for the general science community. Nanoencapsulations of PE gels were first patented in 1957 in the US, but for different purposes, and have caught attention again just recently as drug delivery agents [96, 191]. The application of PE complexes in medical applications, which is currently considered a hot topic, has been investigated since the 1920s in basic science.

Currently PEs play a very important role in many fields of application, where their thermodynamic and rheological properties are most important. Applications which need fine tuned thermodynamic properties include: drug delivery agents,

cosmetics, lubricants, subterrain gelation agent or food itself. The measurement of these thermodynamic properties imposes no problems with current methods.

Recent scaling theories based on the Rouse and Zimm model are able to explain most effects in PEs like the correlation length, viscous effects, counterion condensation and changes in chain length. However, there are still many unexplained effects, like the inability of the scaling theory to correctly explain the modulus and in some cases the relaxation time. Despite interesting MD and MC simulations in this field there is a fundamental mismatch between the length and time scales between macroscopic and microscopic effects of PEs, rendering these methods incapable of explaining macroscopic effects like viscosity (with a few exceptions for very constrained areas and surfaces). To solve such questions, sufficient field based theories are currently being developed.

Although omitted in this chapter, the PE conductivity and osmotic pressure play an important role for daily applications of PE, like the design of ion exchangers where the degree of crosslinking in PE gels is important to resist the high osmotic pressure [191]. Another promising application in regard to PE conductivity is PE gels and PE complex gels which react to electrical stimuli and might serve as artificial muscles.

Acknowledgments Acknowledgments: This work was supported by the National Nature Science Foundation of China (91027045), 100-talent Program of HIT, China Postdoctoral Science Foundation (2013M531019) and New Century Excellent Talent Program (NCET-11-0800) and Harbin Institute of Technology.

References

1. Barrat, J.L., Joanny, J.F.: Theory of polyelectrolyte solutions. In: Prigogine, I., Rice, S.A. (eds.) Advances in Chemical Physics, Polymeric Systems, vol. 94, p. 66. Wiley, Hoboken (1996)
2. Kuhn, W., Künzle, O., Katchalsky, A.: Verhalten polyvalenter Fadenmolekelionen in Lösung. HCA **31**, 1994–2037 (1948). doi:10.1002/hlca.19480310716
3. Manning, G.S.: The molecular theory of polyelectrolyte solutions with applications to the electrostatic properties of polynucleotides. Q. Rev. Biophys. **11**, 179–246 (1978)
4. Jiang, G., Min, S.-H., Hahn, S.K.: DNA/PEI/Alginate polyplex as an efficientin vivo gene delivery system. Biotechnol. Bioprocess Eng. **12**, 684–689 (2007)
5. Hamman, J.H.: Chitosan based polyelectrolyte complexes as potential carrier materials in drug delivery systems. Mar Drugs **8**, 1305–1322 (2010). doi:10.3390/md8041305
6. Decher, G., Schlenoff, J.: Multilayer Thin Films: Sequential Assembly of Nanocomposite Materials, 2nd edn, p. 1112. Wiely, Weinheim (2012)
7. Antonov, Y.A., Moldenaers, P.: Strong polyelectrolyte—induced mixing in concentrated biopolymer aqueous emulsions. Food Hydrocolloids **28**, 213–223 (2012). doi:10.1016/j.foodhyd.2011.12.009
8. Decher, G., Hong, J.D., Schmitt, J.: Build up of ultrathin multilayer films by a self-assembly process: III. Consecutively alternating adsorption of anionic and cationic polyelectrolytes on charged surfaces. Thin Solid Films **210–211**, 831–835 (1992)

9. Caruso, F., Caruso, R.A., Moehwald, H.: Nanoengineering of inorganic and hybrid hollow spheres by colloidal templating. Science **282**(80), 1111–1114 (1998). doi:10.1126/science.282.5391.1111
10. Clasen, C., Kulicke, W.-M.: Determination of viscoelastic and rheo-optical material functions of water-soluble cellulose derivatives. Prog. Polym. Sci. **26**, 1839–1919 (2001). doi:10.1016/S0079-6700(01)00024-7
11. Zhang, L., Huang, S.: Viscosity properties of homogeneous polyelectrolyte complex solutions from sodium carboxymethyl cellulose and poly (acrylamide- co -dimethyldiallylammonium chloride). Polym. Int. **532**, 528–532 (2000)
12. Rehfeldt, F., Tanaka, M.: Hydration forces in ultrathin films of cellulose. Langmuir **19**(5), 1467–1473 (2003)
13. Biermann, O.: Molecular Dynamics Simulation Study of Polyelectrolyte Adsorption on Cellulose Surfaces, p. 163. Universität Dortmund, Dortmund (2001)
14. Berkland, C., Cordova, M., Liang, J.-T., Willhite, G.P.: Polyelectrolyte complexes as delayed gelling agents for oil and gas applications, p. 12 (2008)
15. Osawa, F., Imai, N., Kagawa, I.: Theory of strong polyelectrolyte solutions. J. Polym. Sci. **XIII**, 93–111 (1954)
16. Dobrynin, A.V.: Theory and simulations of charged polymers: from solution properties to polymeric nanomaterials. Curr. Opin. Colloid Interface Sci. **13**, 376–388 (2008)
17. Fuoss, R.M.: Viscosity function for polyelectrolytes. J. Polym. Sci. **3**, 603–604 (1948). doi:10.1002/pol.1948.120030414
18. Borue, V.Y., Erukhimovich, I.Y.: A statistical theory of weakly charged polyelectrolytes: fluctuations, equation of state, and microphase separation. Macromolecules **21**, 3240–3249 (1988)
19. Ou, Z., Muthukumar, M.: Entropy and enthalpy of polyelectrolyte complexation: Langevin dynamics simulations. J. Chem. Phys. **124**, 154902 (2006). doi:10.1063/1.2178803
20. Ariga, K., Ji, Q., Hill, J.P., et al.: Forming nanomaterials as layered functional structures toward materials nanoarchitectonics. NPG Asia Mater. **4**, e17 (2012). doi:10.1038/am.2012.30
21. Schönhoff, M.: Layered polyelectrolyte complexes: physics of formation and molecular properties. Condens. Matter. **15**, 1781–1808 (2003)
22. Gennes, P.G., Pincus, P., Velasco, R.M., Brochard, F.: Remarks on polyelectrolyte conformation. J. Phys. Fr. **37**, 1461–1473 (1976). doi:10.1051/jphys:0197600370120146100
23. Michaeli, I., Overbeek, J.T.G., Voorn, M.J.: Phase separation of polyelectrolyte solutions. J. Polym. Sci. **23**, 443–450 (1957)
24. Dobrynin, A.V., Colby, R.H., Rubinstein, M.: Scaling theory of polyelectrolyte solutions. Macromolecules **28**, 1859–1871 (1995)
25. De Gennes, P.G.: Dynamics of entangled polymer solutions. I. The Rouse model. Macromolecules **9**, 587–593 (1975). doi:10.1021/ma60052a011
26. Dobrynin, A., Rubinstein, M.: Theory of polyelectrolytes in solutions and at surfaces. Prog. Polym. Sci. **30**, 1049–1118 (2005). doi:10.1016/j.progpolymsci.2005.07.006
27. Colby, R.H.: Structure and linear viscoelasticity of flexible polymer solutions: comparison of polyelectrolyte and neutral polymer solutions. Rheol. Acta **49**, 425–442 (2009). doi:10.1007/s00397-009-0413-5
28. De Gennes, P.G.: Dynamics of entangled polymer solutions. II. Inclusion of hydrodynamic interactions. Macromolecules **9**, 594–598 (1976). doi:10.1021/ma60052a012
29. Gennes, P.G.: Scaling Concepts in Polymer Physics. Cornell University Press, Ithaca (1979)
30. Rubinstein, M., Colby, R.H.: Polymer Physics, p. 454. Oxford University, Oxford (2003)
31. Colby, R.H.: Contributions of Nobel Laureate P. G. de Gennes to Polyelectrolyte Solutions, 2008-08-27 (2008)
32. Stramel, R.D., Nguyen, C., Webber, S.E., Rodgers, M.A.J.: Photophysical properties of pyrene covalently bound to photoelectrolytes. J. Chem. Phys. **92**, 2934–2938 (1988)
33. Dong, D.C., Winnik, M.A.: The Py scale of solvent polarities. Can. J. Chem. **62**, 2560–2565 (1984)

34. Winnik, M.A., Bystryak, S.M., Liu, Z., Siddiqui, J.: Synthesis and characterization of pyrene-labeled poly (ethylenimine). Macromolecules **31**, 6855–6864 (1998)
35. Winnik, F.M.: Photophysics of preassociated pyrenes in aqueous polymer solutions and in other organized media. Chem. Rev. **93**, 587–614 (1993)
36. Kundagrami, A., Muthukumar, M.: Theory of competitive counterion adsorption on flexible polyelectrolytes: divalent salts. J. Chem. Phys. **128**, 244901 (2008). doi:10.1063/1.2940199
37. Deshkovski, A., Obukhov, S., Rubinstein, M.: Counterion phase transitions in dilute polyelectrolyte solutions. Phys. Rev. Lett. **86**, 2341–2344 (2001). doi:10.1103/PhysRevLett.86.2341
38. Chang, R., Yethiraj, A.: Brownian dynamics simulations of polyelectrolyte solutions with divalent counterions. J. Chem. Phys. **118**, 11315–11324 (2003). doi:10.1063/1.1575731
39. Frueh, J., Koehler, R., Moehwald, H., Krastev, R.: Changes of the molecular structure in polyelectrolyte multilayers under stress. Langmuir **26**, 15516–15522 (2010). doi:10.1021/la1015324
40. Winnik, M.A., Bystryak, S.M., Liu, Z.: Synthesis and characterization of pyrene-labeled poly (ethylenimine). Macromolecules **9297**, 6855–6864 (1998)
41. Frueh, J., Reiter, G., Möhwald, H., et al.: Orientation change of Polyelectrolytes in linearly elongated polyelectrolyte multilayer measured by polarized UV spectroscopy. Colloid. Surf. A **415**, 366–373 (2012). doi:http://dx.doi.org/10.1016/j.colsurfa.2012.08.070
42. Hinderberger, D., Spiess, H.W., Jeschke, G.: Radial counterion distributions in polyelectrolyte solutions determined by EPR spectroscopy. Europhys. Lett. **70**, 102–108 (2005). doi:10.1209/epl/i2004-10459-y
43. Flory, P.J.: Thermodynamics of high polymer solutions. J. Chem. Phys. **9**, 660 (1941). doi:10.1063/1.1750971
44. Flory, P.J.: Thermodynamics of high polymer solutions. J. Chem. Phys. **51**, 51–61 (1942). doi:10.1063/1.1723621
45. Huggins, M.L.: Solutions of long chain compounds. J. Chem. Phys. **9**, 440 (1941). doi:10.1063/1.1750930
46. Lindvig, T., Michelsen, M.L., Kontogeorgis, G.M.: A Flory-Huggins model based on the Hansen solubility parameters. Fluid Phase Equilib. **203**, 247–260 (2002). doi:10.1016/S0378-3812(02)00184-X
47. Köhler, R., Dönch, I., Ott, P., et al.: Neutron reflectometry study of swelling of polyelectrolyte multilayers in water vapors: influence of charge density of the polycation. Langmuir **25**, 11576–11585 (2009). doi:10.1021/la901508w
48. Frueh, J., Reiter, G., Moehwald, H., et al.: Novel controllable auxetic effect of linearly elongated supported polyelectrolyte multilayer with amorphous structure. Phys. Chem. Chem. Phys. **15**, 483–488 (2013). doi:10.1039/C2CP43302H
49. Safronov, A.P., Zubarev, A.Y.: Flory Huggins parameter of interaction in polyelectrolyle solutions of chitosan and its alkylated derivative. Polymer (Guildf) **43**, 743–748 (2002)
50. Alexander-Katz, A., Leibler, L.: Controlling polyelectrolyte equilibria and structure via counterion–solvent interactions. Soft Matter **5**, 2198 (2009). doi:10.1039/b814653e
51. Hansen, C.M.: Hansen Solubility Paramerters a User's Handbook, 2nd edn, p. 546. CRC Press, Boca Raton (2007)
52. Hansen, C.M.: The Three Dimensional Solubility Parameter and Solvent Diffusion Coefficient, p. 102 (1967)
53. Pfeuty, P., Velasco, R.M., DE Gennes, P.G.: Conformation properties of one isolated polyelectrolyte chain in D dimensions. LE J. Phys. **38**, 5–7 (1977)
54. Tsonchev, S., Coalson, R.D., Duncan, A.: Statistical mechanics of charged polymers in electrolyte solutions: a lattice field theory approach. Phys. Rev. E **60**, 4257–4267 (1999)
55. Bungenberg, D.E., Jong, H.G., Kruyt, H.R.: Coacewation (Partial Miscibility in Colloid Systems). Chemistry (Easton), p. 9. DWC, Utrecht (1929)
56. Skerjanc, J.: Heats of dilution of polyacrylic acid at various degrees of ionization. Biophys. Chem. **1**, 376–380 (1974). doi:10.1016/0301-4622(74)85007-6

57. Godec, A., Skerjanc, J.: Enthalpy changes upon dilution and ionization of poly(L-glutamic acid) in aqueous solutions. J. Phys. Chem. B **109**, 13363–13367 (2005). doi:10.1021/jp050234a
58. Alfrey, T., Berg, P.W., Morawetz, H.: The counterion distribution in solutions of rod-shaped polyelectrolytes. J. Polym. Sci. **VII**, 543–547 (1951)
59. Muthukumar, M.: Theory of counter-ion condensation on flexible polyelectrolytes: adsorption mechanism. J. Chem. Phys. **120**, 9343–9350 (2004). doi:10.1063/1.1701839
60. Kagawa, I., Nagasawa, M.: Statistical thermodynamics. J. Polym. Sci. **XVI**, 299–310 (1955)
61. Mandel, M.: Statistical thermodynamics of polyelectrolyte solutions. In: Selegny, E. (ed.) Polyelectrolytes, pp. 39–55. D. Reidel Publishing Company, Dordrecht (1974)
62. Overbeek, J.T., Voorn, M.J.: Phase separation in polyelectrolyte solutions; theory of complex coacervation. J. Cell Physiol. Suppl. **49**, 7–22 (1957). (discussion, 22–6)
63. Schlenoff, J.B., Rmaile, A.H., Bucur, C.B.: Hydration contributions to association in polyelectrolyte multilayers and complexes: visualizing hydrophobicity. J. Am. Chem. Soc. **130**, 13589–13597 (2008). doi:10.1021/ja802054k
64. Von Solms, N., Chiew, Y.C.: Analytical integral equation theory for a restricted primitive model of polyelectrolytes and counterions within the mean spherical approximation. II. Radial distribution functions. J. Chem. Phys. **118**, 4321 (2003). doi:10.1063/1.1539842
65. Bekturov, E.A., Bimend, L.A.: Interpolymer complexes. In: Dusek, K. (ed.) Advances in Polymer Science, vol. 41, pp. 99–147. Springer, Berlin (1980)
66. Feng, X., Leduc, M., Pelton, R.: Polyelectrolyte complex characterization with isothermal titration calorimetry and colloid titration. Colloids Surf. A Physicochem. Eng. Asp. **317**, 535–542 (2008). doi:10.1016/j.colsurfa.2007.11.053
67. Nyström, R., Hedström, G., Gustafsson, J., Rosenholm, J.B.: Mixtures of cationic starch and anionic polyacrylate used for flocculation of calcium carbonate—influence of electrolytes. Colloids Surf. A Physicochem. Eng. Asp. **234**, 85–93 (2004). doi:10.1016/j.colsurfa.2003.12.012
68. Steitz, R., Jaeger, W., Klitzing, Rv: Influence of charge density and ionic strength on the multilayer formation of strong polyelectrolytes. Langmuir **17**, 4471–4474 (2001)
69. Klitzing, Rv: Internal structure of polyelectrolyte multilayer assemblies. Phys. Chem. Chem. Phys. **8**, 5012–5033 (2006)
70. Köhler, K., Shchukin, D.G., Möhwald, H., Sukhorukov, G.B.: Thermal behavior of polyelectrolyte multilayer microcapsules. 1. The effect of odd and even layer number. J. Phys. Chem. B **109**, 18250–18259 (2005). doi:10.1021/jp052208i
71. Köhler, K., Biesheuvel, P., Weinkamer, R., et al.: Salt-induced swelling-to-shrinking transition in polyelectrolyte multilayer capsules. Phys. Rev. Lett. **97**, 3–6 (2006). doi:10.1103/PhysRevLett.97.188301
72. Hugerth, A., Caram-Lelham, N., Sundeloef, L.-O.: The effect of charge density and conformation on the polyelectrolyte complex formation between carrageenan and chitosan. Carbohydr. Poiymers **34**, 149–156 (1997)
73. Kazuo, H., Akashi, S., Furuya, M., Fukuhara, K.: Rapid confirmation and revision of the primary structure of bovine serum albumin by ESIMS and frit-FAB LC/MS. Biochem. Biophys. Res. Commun. **173**, 639–646 (1990)
74. Baeurle, Sa: Multiscale modeling of polymer materials using field-theoretic methodologies: a survey about recent developments. J. Math. Chem. **46**, 363–426 (2009). doi:10.1007/s10910-008-9467-3
75. Baeurle, Sa: Grand canonical auxiliary field Monte Carlo: a new technique for simulating open systems at high density. Comput. Phys. Commun. **157**, 201–206 (2004). doi:10.1016/j.comphy.2003.11.001
76. Baeurle, S., Charlot, M., Nogovitsin, E.: Grand canonical investigations of prototypical polyelectrolyte models beyond the mean field level of approximation. Phys. Rev. E **75**, 011804 (2007). doi:10.1103/PhysRevE.75.011804

77. Baeurle, Sa, Nogovitsin, Ea: Challenging scaling laws of flexible polyelectrolyte solutions with effective renormalization concepts. Polymer (Guildf) **48**, 4883–4899 (2007). doi:10.1016/j.polymer.2007.05.080
78. Peter, E., Dick, B., Baeurle, Sa: A novel computer simulation method for simulating the multiscale transduction dynamics of signal proteins. J. Chem. Phys. **136**, 124112 (2012). doi:10.1063/1.3697370
79. Donets, S., Pershin, A., Christlmaier, M.J., Baeurle, Sa: A multiscale modeling study of loss processes in block-copolymer-based solar cell nanodevices. J. Chem. Phys. **138**, 094901 (2013). doi:10.1063/1.4792366
80. Kuhn, W.: Über die Gestalt fadenförmiger Molekiile in Lösungen. Kolloid-Z **68**, 2–15 (1934)
81. Patra, C.N., Yethiraj, A.: Density functional theory for the distribution of small ions around polyions. J. Phys. Chem. B **103**, 6080–6087 (1999). doi:10.1021/jp991062i
82. Ermoshkin, A.V., Cruz, M.: Gelation in strongly charged polyelectrolytes. J Polym Sci **42**, 766–776 (2004). doi:10.1002/polb.10752
83. Ermoshkin, a, Olvera de la Cruz, M.: Polyelectrolytes in the presence of multivalent ions: gelation versus segregation. Phys. Rev. Lett. **90**, 125504 (2003). doi:10.1103/PhysRevLett.90.125504
84. Deshkovski, A., Obukhov, S., Rubinstein, M.: Counterion phase transitions in dilute polyelectrolyte solutions. Phys. Rev. Lett. **86**, 2341–2344 (2001). doi:10.1103/PhysRevLett.86.2341
85. Mjahed, H., Voegel, J.-C., Senger, B., et al.: Hole formation induced by ionic strength increase in exponentially growing multilayer films. Soft Matter **5**, 2269 (2009). doi:10.1039/b819066f
86. Netz, R.R., Andelman, D.: Polyelectrolytes in solution and at surfaces. In: Bard, A., Stratmann, M. (eds.) Encyclopedia of Electrochemistry, vol. 1, pp. 282–322. Wiley-VCH Verlag GmbH & Co, KGaA, Weinheim (2002)
87. Adam, M., Delsanti, M.: Viscosity and longest relaxation time of semi-dilute polymer solutions. I. Good Solvent. J Phys **44**, 1185–1193 (1983)
88. Adam, M., Delsanti, M.: Viscosity and longest relaxation time of semi-dilute polymer solutions: II. Theta Solvent. J. Phys. **45**, 1513–1521 (1984)
89. Pfeuty, P.: Conformation des polyelectrolytes ordre dans les solutions de polyelectrolytes. J. Phys. **39**, C2–149–C2–160 (1978). doi:10.1051/jphyscol:1978227
90. Rubinstein, M., Colby, R., Dobrynin, A.: Dynamics of semidilute polyelectrolyte solutions. Phys. Rev. Lett. **73**, 2776–2779 (1994)
91. Kavassalis, T., Noolandi, J.: New view of entanglements in dense polymer systems. Phys. Rev. Lett. **59**, 2674–2677 (1987)
92. Kavassalis, T.A., Noolandi, J.: A new theory of entanglements and dynamics in dense polymer systems. Macromolecules **21**, 2869–2879 (1988)
93. Kavassalis, T.A., Noolandi, J.: Entanglement scaling in polymer melts and solutions. Macromolecules **2720**, 2709–2720 (1989)
94. Dobrynin, A.V., Rubinstein, M.: Hydrophobic polyelectrolytes. Macromolecules **32**, 915–922 (1999). doi:10.1021/ma981412j
95. Dobrynin, A.V., Rubinstein, M.: Counterion condensation and phase separation in solutions of hydrophobic polyelectrolytes. Macromolecules **34**, 1964–1972 (2001)
96. Kwon, H.J., Osada, Y., Gong, J.P.: Polyelectrolyte gels-fundamentals and applications. Polym. J. **38**, 1211–1219 (2006). doi:10.1295/polymj.PJ2006125
97. Ermoshkin, aV, Kudlay, aN, Olvera de la Cruz, M.: Thermoreversible crosslinking of polyelectrolyte chains. J. Chem. Phys. **120**, 11930–11940 (2004). doi:10.1063/1.1753573
98. Kudlay, A., Ermoshkin, A.V., Olvera de la Cruz, M.: Complexation of oppositely charged polyelectrolytes: effect of ion pair formation. Macromolecules **37**, 9231–9241 (2004). doi:10.1021/ma048519t
99. Gibaud, A., Hazra, S.: X-ray reflectivity and diffuse scattering. Curr. Sci. **78**, 11 (2000)

100. Dietrich, S., Haase, A.: Scattering of X-rays and neutrons at interfaces. Phys. Rep. **260**, 1–138 (1995)
101. Alder, B.J., Wainwright, T.E.: Studies in molecular dynamics. I. General Method. J Chem Phys **31**, 459 (1959). doi:10.1063/1.1730376
102. Metropolis, N., Rosenbluth, A.W., Rosenbluth, M.N., et al.: Equation of state calculations by fast computing machines. J. Chem. Phys. **21**, 1087 (1953). doi:10.1063/1.1699114
103. Müller-Plathe, F.: Coarse-graining in polymer simulation: from the atomistic to the mesoscopic scale and back. Chem. Phys. Chem. **3**, 755–769 (2002)
104. Peter, C., Kremer, K.: Multiscale simulation of soft matter systems—from the atomistic to the coarse-grained level and back. Soft Matter **5**, 4357 (2009). doi:10.1039/b912027k
105. Feynman, R.P.: Simulating physics with computers. Int. J. Theor. Phys. **21**, 467–488 (1982). doi:10.1007/BF02650179
106. Simon, D.R.: On the power of quantum computation. In: Proceedings 35th Annual Symposium on Foundations of Computer Science, pp. 116–123. Santa Fe, NM (1994)
107. D-wave.: D-wave company homepage. Homepage http://www.dwavesys.com/en/dw_homepage.html (2013). Accessed 30 Jul 2013
108. Perdomo-Ortiz, A., Dickson, N., Drew-Brook, M., et al.: Finding low-energy conformations of lattice protein models by quantum annealing. Sci. Rep. **2**, 571 (2012). doi:10.1038/srep00571
109. De Pablo, J.J.: Coarse-grained simulations of macromolecules: from DNA to nanocomposites. Annu. Rev. Phys. Chem. **62**, 555–574 (2011). doi:10.1146/annurev-physchem-032210-103458
110. Bouvard, J.L., Ward, D.K., Hossain, D., et al.: Review of hierarchical multiscale modeling to describe the mechanical behavior of amorphous polymers. J. Eng. Mater. Technol. **131**, 041206 (2009). doi:10.1115/1.3183779
111. Pierleoni, C., Ryckaert, J.-P.: Deformation and orientation of flexible polymers in solution under shear flow: a new picture for intermediate reduced shear rates. Macromolecules **28**, 5097–5108 (1995). doi:10.1021/ma00118a044
112. Carrillo, J.-M.Y., Russano, D., Dobrynin, A.V.: Friction between brush layers of charged and neutral bottle-brush macromolecules. Molecular dynamics simulations. Langmuir **27**, 14599–14608 (2011). doi:10.1021/la203525r
113. Radeva, T.: Physical Chemistry of Polyelectrolytes, p. 936. CRC Press, Boca Raton (2001)
114. Alarcón, F., Pérez-Hernández, G., Pérez, E., Gama Goicochea, a: Coarse-grained simulations of the salt dependence of the radius of gyration of polyelectrolytes as models for biomolecules in aqueous solution. Eur. Biophys. J. **42**, 661–672 (2013). doi:10.1007/s00249-013-0915-z
115. Dobrynin, a: Theory and simulations of charged polymers: From solution properties to polymeric nanomaterials. Curr. Opin. Colloid Interface Sci. **13**, 376–388 (2008). doi:10.1016/j.cocis.2008.03.006
116. Da Silva, F.L.B., Lund, M., Jönsson, B., Akesson, T.: On the complexation of proteins and polyelectrolytes. J. Phys. Chem. B **110**, 4459–4464 (2006). doi:10.1021/jp054880l
117. Edgecombe, S., Linse, P.: Monte Carlo simulations of cross-linked polyelectrolyte gels with oppositely charged macroions. Langmuir **22**, 3836–3843 (2006). doi:10.1021/la053193i
118. Edgecombe, S., Linse, P.: Monte Carlo simulation of polyelectrolyte gels: effects of polydispersity and topological defects. Macromolecules **40**, 3868–3875 (2007). doi:10.1021/ma0700633
119. Carrillo, J.-M.Y., Dobrynin, A.V.: Detailed molecular dynamics simulations of a model NaPSS in water. J. Phys. Chem. B **114**, 9391–9399 (2010). doi:10.1021/jp101978k
120. Detcheverry, Fa, Pike, D.Q., Nagpal, U., et al.: Theoretically informed coarse grain simulations of block copolymer melts: method and applications. Soft Matter **5**, 4858 (2009). doi:10.1039/b911646j
121. Becker, N., Everaers, R.: From rigid base pairs to semiflexible polymers: Coarse-graining DNA. Phys. Rev. E **76**, 021923 (2007). doi:10.1103/PhysRevE.76.021923

122. Chang, R., Yethiraj, A.: Strongly charged flexible polyelectrolytes in poor solvents: molecular dynamics simulations with explicit solvent. J. Chem. Phys. **118**, 6634 (2003). doi:10.1063/1.1558312
123. Ou, Z., Muthukumar, M.: Langevin dynamics of semiflexible polyelectrolytes: rod-toroid-globule-coil structures and counterion distribution. J. Chem. Phys. **123**, 074905 (2005). doi:10.1063/1.1940054
124. Liao, Q., Dobrynin, A.V., Rubinstein, M.: Counterion-correlation-induced attraction and necklace formation in polyelectrolyte solutions: theory and simulations. Macromolecules **39**, 1920–1938 (2006)
125. Stevens, M.J., Kremer, K.: The nature of flexible linear polyelectrolytes in salt free solution: a molecular dynamics study. J. Chem. Phys. **103**, 1669 (1995). doi:10.1063/1.470698
126. Micka, U., Holm, C., Kremer, K.: Strongly charged solvents: flexible polyelectrolytes in poor solvents: molecular dynamics simulations. Langmuir **15**, 4033–4044 (1999)
127. Limbach, H.J., Holm, C.: End effects of strongly charged polyelectrolytes: a molecular dynamics study. J. Chem. Phys. **114**, 9674 (2001). doi:10.1063/1.1370077
128. Liao, Q., Dobrynin, A.V., Rubinstein, M.: Molecular dynamics simulations of polyelectrolyte solutions: nonuniform stretching of chains and scaling behavior. Macromol. **36**, 3386–3398 (2003). doi:10.1021/ma025995f
129. Sandberg, D.J., Carrillo, J.-M.Y., Dobrynin, A.V.: Molecular dynamics simulations of polyelectrolyte brushes: from single chains to bundles of chains. Langmuir **23**, 12716–12728 (2007). doi:10.1021/la702203c
130. Russano, D., Carrillo, J.-M.Y., Dobrynin, A.V.: Interaction between brush layers of bottle-brush polyelectrolytes: molecular dynamics simulations. Langmuir **27**, 11044–11051 (2011). doi:10.1021/la2018067
131. Micka, U., Kremer, K.: Strongly charged flexible polyelectrolytes in poor solvents-from stable spheres to necklace chains. Eur. Lett. **49**, 189–195 (2000)
132. Limbach, H.J., Holm, C.: Conformational properties of poor solvent polyelectrolytes. Comput. Phys. Commun. **147**, 321–324 (2002). doi:10.1016/S0010-4655(02)00295-3
133. Limbach, H.J., Holm, C., Kremer, K.: Structure of polyelectrolytes in poor solvent. Eur. Lett. **60**, 566–572 (2002)
134. Limbach, H.J., Holm, C., Kremer, K.: Conformations and solution structure of polyelectrolytes in poor solvent. Macromol. Symp. **211**, 43–54 (2004). doi:10.1002/masy.200450703
135. Limbach, H.J., Holm, C.: Single-chain properties of polyelectrolytes in poor solvent. J. Phys. Chem. B **107**, 8041–8055 (2003)
136. Jeon, J., Dobrynin, A.V.: Necklace globule and counterion condensation. Macromolecules **40**, 7695–7706 (2007). doi:10.1021/ma071005k
137. Wang, Z., Rubinstein, M.: Regimes of conformational transitions of a diblock polyampholyte. Macromolecules **39**, 5897–5912 (2006). doi:10.1021/ma0607517
138. Carrillo, J.-M.Y., Dobrynin, A.V.: Polyelectrolytes in salt solutions: molecular dynamics simulations. Macromolecules **44**, 5798–5816 (2011). doi:10.1021/ma2007943
139. Konieczny, M., Likos, C.N., Löwen, H.: Soft effective interactions between weakly charged polyelectrolyte chains. J. Chem. Phys. **121**, 4913–4924 (2004). doi:10.1063/1.1781111
140. Jeon, J., Dobrynin, A.V.: Molecular dynamics simulations of polyampholyte-polyelectrolyte complexes in solutions. Macromolecules **38**, 5300–5312 (2005)
141. Jeon, J., Dobrynin, A.V.: Molecular dynamics simulations of polyelectrolyte-polyampholyte complexes. Effect of solvent quality and salt concentration. J. Phys. Chem. B **110**, 24652–24665 (2006). doi:10.1021/jp064288b
142. Jeon, J., Panchagnula, V., Pan, J., Dobrynin, A.V.: Molecular dynamics simulations of multilayer films of polyelectrolytes and nanoparticles. Langmuir **22**, 4629–4637 (2006). doi:10.1021/la053444n
143. Patel, Pa, Jeon, J., Mather, P.T., Dobrynin, A.V.: Molecular dynamics simulations of layer-by-layer assembly of polyelectrolytes at charged surfaces: effects of chain degree of

polymerization and fraction of charged monomers. Langmuir **21**, 6113–6122 (2005). doi:10.1021/la050432t
144. Patel, Pa, Jeon, J., Mather, P.T., Dobrynin, A.V.: Molecular dynamics simulations of multilayer polyelectrolyte films: effect of electrostatic and short-range interactions. Langmuir **22**, 9994–10002 (2006). doi:10.1021/la061658e
145. Carrillo, J.-M.Y., Dobrynin, A.V.: Molecular dynamics simulations of polyelectrolyte adsorption. Langmuir **23**, 2472–2482 (2007). doi:10.1021/la063079f
146. Carrillo, J.-M.Y., Dobrynin, A.V.: Layer-by-layer assembly of polyelectrolyte chains and nanoparticles on nanoporous substrates: molecular dynamics simulations. Langmuir **28**, 1531–1538 (2012). doi:10.1021/la203940w
147. Mann, Ba, Holm, C., Kremer, K.: Swelling of polyelectrolyte networks. J. Chem. Phys. **122**, 154903 (2005). doi:10.1063/1.1882275
148. Mann, Ba, Everaers, R., Holm, C., Kremer, K.: Scaling in polyelectrolyte networks. Europhys. Lett. **67**, 786–792 (2004). doi:10.1209/epl/i2004-10121-x
149. Lu, Z.-Y., Hentschke, R.: Computer simulation study on the swelling of a polyelectrolyte gel by a Stockmayer solvent. Phys. Rev. E **67**, 061807 (2003). doi:10.1103/PhysRevE.67.061807
150. Liao, Q., Carrillo, J.Y., Dobrynin, A.V., Rubinstein, M.: Rouse dynamics of polyelectrolyte solutions: molecular dynamics study. Macromolecules **40**, 7671–7679 (2007)
151. Zhou, T., Chen, S.B.: Computer simulations of diffusion and dynamics of short-chain polyelectrolytes. J. Chem. Phys. **124**, 034904 (2006). doi:10.1063/1.2161205
152. Krause, W.E., Tan, J.S., Colby, R.H.: Semidilute solution rheology of polyelectrolytes with no added salt. J. Polym. Sci. B **37**, 3429–3437 (1999). doi:10.1002/(SICI)1099-0488(19991215)37:24<3429:AID-POLB5>3.0.CO;2-E
153. Yin, D.-W., Yan, Q., de Pablo, J.J.: Molecular dynamics simulation of discontinuous volume phase transitions in highly-charged crosslinked polyelectrolyte networks with explicit counterions in good solvent. J. Chem. Phys. **123**, 174909 (2005). doi:10.1063/1.2102827
154. Sun, F., Dobrynin, A., Shirvanyants, D., et al.: Flory theorem for structurally asymmetric mixtures. Phys. Rev. Lett. **99**, 137801 (2007). doi:10.1103/PhysRevLett.99.137801
155. Heidelberger, M., Kendall, F.E.: Some physicochemical properties of specific polysaccharides. J. Biol. Chem. **95**, 127–142 (1932)
156. Staudinger, H.: Die hochmolekularen organischen Verbindungen. **540** (1932). doi:10.1002/bbpc.19320381231
157. Staudinger, H.: Der Aufbau der hochmolekularen organischen Verbindungen. Naturwissenschaften **22**, 65–71 (1934)
158. Fuoss, R.M., Strauss, U.P.: Polyelectrolytes. II. Poly-4-vinylpyridonium chloride and poly-4-vinyl-N-n-butylpyridonium bromide. J Polym Sci **3**, 246–263 (1948). doi:10.1002/pol.1948.120030211
159. Cohen, J., Priel, Z., Rabin, Y.: Viscosity of dilute polyelectrolyte solutions. J. Chem. Phys. **88**, 7111 (1988). doi:10.1063/1.454361
160. Terayama, H., Wall, F.T.: Reduced viscosities of polyelectrolytes in the presence of added salts. J. Polym. Sci. **XVI**, 357–365 (1955). doi:10.1002/pol.1955.120168224
161. Prini, R.F., Lagos, A.E.: Tracer diffusion, electrical conductivity, and viscosity of aqueous solutions of poly styrenesulfonates. J. Polym. Sci. A **2**, 2917–2928 (1964). doi:10.1002/pol.1964.100020640
162. Zebrowski, B.E.: Rheo-optical studies of polyelectrolyte solutions in simple shear flow. J. Rheol. (N Y N Y) **29**, 943 (1985). doi:10.1122/1.549823
163. Zimm, B.H.: Dynamics of polymer molecules in dilute solution: viscoelasticity, flow birefringence and dielectric loss. J. Chem. Phys. **24**, 269 (1956). doi:10.1063/1.1742462
164. Boris, D.C., Colby, R.H.: Rheology of sulfonated polystyrene solutions. Macromolecules **31**, 5746–5755 (1998)
165. Colby, R.H., Boris, D.C., Krause, W.E., Dou, S.: Shear thinning of unentangled flexible polymer liquids. Rheol. Acta **46**, 569–575 (2007). doi:10.1007/s00397-006-0142-y

166. Chen, S., Archer, L.A.: Relaxation dynamics of salt-free polyelectrolyte solutions using flow birefringence and rheometry. J. Polym. Sci. B **37**, 825–835 (1998). doi:10.1002/(SICI)1099-0488(19990415)37:8<825:AID-POLB8>3.0.CO;2-H/pdf
167. Dou, S., Colby, R.H.: Charge density effects in salt-free polyelectrolyte solution rheology. J. Polym. Sci. Part B **44**, 2001–2013 (2006). doi:10.1002/polb
168. Di Cola, E., Plucktaveesak, N., Waigh, Ta, et al.: Structure and dynamics in aqueous solutions of amphiphilic sodium maleate-containing alternating copolymers. Macromolecules **37**, 8457–8465 (2004). doi:10.1021/ma049260h
169. Strauss, U.P., Smith, E.H., Winema, P.L.: Polyphosphates as polyelectrolytes. I. Light scattering and viscosity of sodium. J. Am. Chem. Soc. **75**, 3935–3940 (1953). doi:10.1021/ja01112a017
170. Strauss, U.P., Smith, E.H.: Polyphosphates as polyelectrolytes. II. Viscosity of aqueous solutions of Graham's salts. JACS **75**, 6186–6188 (1953). doi:10.1021/ja01120a023
171. Nierlich, M., Williams, C.E., Boué, F., et al.: Small angle neutron scattering by semi-dilute solutions of polyelectrolyte. J. Phys. **40**, 701–704 (1979). doi:10.1051/jphys:01979004007070100
172. Williams, C.E., Nierlich, M., Cotton, J.P., et al.: Polyelectrolyte solutions: intrachain and interchain correlations observed by SANS. J. Polym. Sci. Polym. Lett. Ed. **17**, 379–384 (1979). doi:10.1002/pol.1979.130170608
173. Essafi, W., Lafuma, F., Williams, C.E.: Structural evidence of charge renormalization in semi-dilute solutions of highly charged polyelectrolytes. Eur. Phys. J. B **9**, 261–266 (1999). doi:10.1007/s100510050765
174. Bordi, F., Cametti, C., Tan, J.S., et al.: Determination of polyelectrolyte charge and interaction with water using dielectric spectroscopy. Macromolecules **35**, 7031–7038 (2002). doi:10.1021/ma020116a
175. Lösche, M., Schmitt, J., Decher, G., et al.: Detailed structure of molecularly thin polyelectrolyte multilayer films on solid substrates as revealed by neutron reflectometry. Macromolecules **31**, 8893–8906 (1998). doi:10.1021/ma980910p
176. Drifford, M., Dalbiez, J.-P.: Light scattering by dilute solutions of salt-free polyelectrolytes. J. Phys. Chem. **88**, 5368–5375 (1984)
177. Park, J., Hammond, P.T.: Polyelectrolyte multilayer formation on neutral hydrophobic surfaces. Macromolecules **38**, 10542–10550 (2005)
178. Ito, K., Yagi, A., Ookubo, N., Hayakawa, R.: Crossover behavior in high-frequency dielectric relaxation of linear polyions in dilute and semidilute solutions. Macromolecules **23**, 857–862 (1990). doi:10.1021/ma00205a027
179. Bordi, F., Cametti, C., Sennato, S., et al.: Dielectric scaling in polyelectrolyte solutions with different solvent quality in the dilute concentration regime. Phys. Chem. Chem. Phys. **8**, 3653–3658 (2006). doi:10.1039/b605624e
180. Marudova, M., Rashkov, I.: Pectin and its polyelectrolyte complexes in food coating and encapsulation of food-stuffs. Internet **15**
181. Müller, M., Keßler, B., Fröhlich, J., et al.: Polyelectrolyte complex nanoparticles of poly(ethyleneimine) and poly(acrylic acid): preparation and applications. Polymers (Basel) **3**, 762–778 (2011). doi:10.3390/polym3020762
182. Hariri, H.H., Lehaf, A.M., Schlenoff, J.B.: Mechanical properties of osmotically stressed polyelectrolyte complexes and multilayers: water as a plasticizer. Macromolecules **45**, 9364–9372 (2012). doi:10.1021/ma302055m
183. Frueh, J., Nakashima, N., He, Q., Moehwald, H.: Effect of linear elongation on carbon nanotube and polyelectrolyte structures in PDMS-supported nanocomposite LbL films. J Phys Chem B **116**, 12257–12262 (2012). doi:10.1021/jp3071458
184. Dumitriu, S., Magny, P., Montane, D., et al.: Polyionic hydrogels obtained by complexation between Xanthan and Chitosan: their properties as supports for enzyme immobilization. J. Bioact. Compat. Polym. **9**, 184–209 (1994). doi:10.1177/088391159400900205
185. Soares, A.F., Oliveira, L.M., Reis, C., Veiga, F.: Characterization of polyelectrolyte interactions of alginate core nanospheres coated with polyelectrolytes and acid-protective

biomaterials for oral insulin delivery. In: XVth International Workshop on Bioencapsulation, Vienna, Au. 6–8 Sept 2007, pp 10–13. Impascience.eu, Vienna (2007)
186. Kasper, J.C., Pikal, M.J., Friess, W.: Investigations on polyplex stability during the freezing step of lyophilization using controlled ice nucleation—the importance of residence time in the low-viscosity fluid state. J. Pharm. Sci. **102**, 9–11 (2012). doi:10.1002/jps
187. Danielsen, S., Maurstad, G., Stokke, B.T.: DNA-polycation complexation and polyplex stability in the presence of competing polyanions. Biopolymers **77**, 86–97 (2004). doi:10.1002/bip.20170
188. Ho, Y.-P., Chen, H.H., Leong, K.W., Wang, T.-H.: The convergence of quantum-dot-mediated fluorescence resonance energy transfer and microfluidics for monitoring DNA polyplex self-assembly in real time. Nanotechnology **20**, 095103 (2009). doi:10.1088/0957-4484/20/9/095103
189. Magnin, D.: Physicochemical and structural characterization of a polyionic matrix of interest in biotechnology, in the pharmaceutical and biomedical fields. Carbohydr. Polym. **55**, 437–453 (2004). doi:10.1016/j.carbpol.2003.11.013
190. Ermoshkin, A.V., Cruz, M.: Gelation in strongly charged polyelectrolytes*. J. Polym. Sci. Part B **42**, 766–776 (2004)
191. Overbeek, J.T.G.: Polyelectrolytes, past, present and future. Pure Appl. Chem. **46**, 91–101 (1976). doi:10.1351/pac197646020091

Springer

http://www.springer.com/978-3-319-01679-5

Polyelectrolytes
Thermodynamics and Rheology
P. M., V.; Bayraktar, O.; Picó, G. (Eds.)
2014, XII, 379 p. 146 illus., 37 illus. in color., Hardcover
ISBN: 978-3-319-01679-5